UNIVERSITY OF MISKOLC
FACULTY OF MECHANICAL ENGINEERING AND INFORMATICS

DETECTION OF THE DAMAGES OF COMPOSITE MACHINE AND VEHICLE STRUCTURES WITH ACOUSTIC METHODS

PHD THESES

Prepared by

Saad Jabber Nazal Alsarayefi
Engineering of Mechanics … (BSc),
Engineering of Mechanics/ Design … (MSc)

ISTVÁN SÁLYI DOCTORAL SCHOOL OF MECHANICAL ENGINEERING SCIENCES
TOPIC FIELD OF DESIGN OF MACHINES AND STRUCTURES
TOPIC GROUP OF DESIGN OF MACHINES AND ELEMENTS

Head of Doctoral School

Dr. Gabriella Bognár Vadászné
DSc, Full Professor

Head of Topic Group

Dr. Gabriella Bognár Vadászné

Scientific Supervisor

Dr. Gabriella Bognár Vadászné
Dr. Károly Jálics

Miskolc
2022

CONTENTS

LIST OF FIGURES

LIST OF TABLES

LIST OF SYMBOLS AND ABBREVIATIONS

SUPERVISOR'S RECOMMENDATIONS

PhD candidate Saad Jabber Nazal Alsarayefi has been under our supervision for the last 5 years.
From September 2017 to August 2021, he was a full-time PhD student at the Sályi István Sályi Doctoral School of Mechanical Engineering, in the framework of the "Stipendium Hungaricum Scholarship Programme", affiliated to the Institute of Mechanical and Product Design / Faculty of Mechanical Engineering and Information Technology. He was awarded a one-year extension of the fellowship from 2021 to the present. His research work on the detection of damage in composite materials by acoustic methods is a very important and active research area in the automotive and aviation industries today. An increasing number of vehicle and aircraft components are made of composite structures, which has a cost and safety dimension. For this reason, well-timed damage detection can save costs and, not exaggeratedly, lives.

The results of candidate's research work were continuously published and presented in scientific journals, in doctoral seminars, doctoral forums, and international conferences, and in conference proceedings. The work has the possibility for extension, since there are further questions which occurred during the work, and which could not be answered within the scope of the work.
In 2019, he successfully passed the complex examination with 100% in the theoretical part and 86.6% in the thesis part.On 5 March 2021, he received his undergraduate degree from the doctoral school with 278.5 credits. The departmental examination was successfully completed on 8 June 2022.
The candidate often worked independently and proactively, always following instructions. During his doctoral studies, he continued to develop his knowledge, affinity for research and ability to deliver presentations. He has acquired new knowledge and competences that he will be able to use in his future academic life.

Miskolc. 14.06.2022

Gabriella Vadászné Bognár	Jálics Károly
Prof. Dr.	PhD.

1. INTRODUCTION, GLOBAL AIM OF THE RESEARCH WORK

A composite material is a combination of two or more distinct materials that formed to have enhanced mechanical properties and performance that are superior to those of the constituents if they act individually. One of the combined materials is called the reinforcement which is stiffer and stronger while the other one is called the matrix. The insured advantageous properties of composite materials have steadily extended their use in various fields of engineering.

Composite materials usages have been remarkably increased in almost all industry sectors. Fiber reinforced polymer (FRP) composites in particular, are significantly adopted in aerospace and automobile structures to satisfy the need for materials that are light in weight, costly effective, and good impact absorbents [1]. Fiber reinforced polymer (FRP) is a major class of composite materials that generally consists of a polymer as a matrix reinforced with a fiber. Usually, the fiber might be glass, carbon, and Kevlar. However, other types of fiber sometimes are used such as wood, paper, or asbestos etc. [2].

Branched from the two main categories, thermoplastics and thermoset, polymer also could be of many types such as polyester, vinylester, polyurethane, and epoxy. Due to commercial needs, Glass or carbon is the most commonly used fibers as reinforcement to a matrix of thermosetting polymer such as epoxy and polyester to have FRP composite materials [3, 4]. Moreover, thermoplastics matrices are still preferred to be used because of their property of reformed after the initial production. Regarding the application of FRP composites, their usage is remarkable in the aerospace and automobile industry field, ships and offshores platforms, sport goods, and chemical processing equipment. Also, FRP composite have exist in new markets of biomedical devices and civil structures.

New style of reinforcement forms such as carbon nanotube and nanoparticles with high performance resin systems have been used to produce new advanced forms of FRP composite rising their usage to an impressive range [5].

Generally, the most important properties of FRP composites that making them attractive to industries sectors are high specific strength, high specific stiffness, high fracture resistance, good abrasion, corrosion, impact, and fatigue resistance, and low cost [6].

On the other hand, damages may arise in the FRP components during operation putting the structure in a risk [7]. Due to the heterogeneous microstructure of the materials and big difference of the constituent's properties, the mechanism of the damage is not smoothly predicted and understood. Also, the interface presence and the fiber orientations give anisotropy in overall properties of the materials [7, 8].

The diagnosed damages of composite materials are broadly classified under three main categories based on the structure of the material. These main categories are the micro-structure level, the macro-structure level, and the coupled micro-macro level mechanism failure. Under all three levels, the damages of composite materials could be [9]:

- Fiber Fracture
- Fiber Bending
- Fiber Buckling
- Matrix Cracking
- Delamination
- Fiber-Matrix Debonding
- others

Fiber reinforced polymers (FRP) are more and more utilized in the vehicle and machine industry. FRP components can show damages that are not visible after impact, crash.
A component that is not visibly damaged loses its load capacity or its original energy absorption capacity. This can lead to undefined component failure during further load. A recorded failure history can provide important information concerning a possible propagation of damages to complete failure. Damaged FRP components can be detected and replaced by means of damage detection methods. Costs can be reduced, because components no longer have to be replaced as a precautionary measure.
In order to have an early prediction of existence of visible or non-visible damages in composite structure and avoid failure, many structural health monitoring (SHM) methods have been revealed. Among these methods are guided waves method, acoustic emission methods, wave field imaging, modal analysis, frequency response function method, and others [9, 10]. Thus, a lot of attention has been paid to the issue of damages detection in composite materials structures using acoustic emission and vibration-based methods.
The global aim of this work is to the identification and tracking of non-visible damage (delamination, fiber and matrix fractures) due to a test bench load using online and/or offline acoustic based measurements.

2. COMPOSITE MATERIALS

2.1. *Historical Overview*

There were remarkable uses of composite materials during the ancient time. For example, back to 1500 BC, straw reinforced walls were introduced for the first time as a composite material by Mesopotamians and Egyptians. Also, there were chariots made of glued layers of wood, bone and horn. A laminated writing material from the papyrus plant was made [11].

After the BC era, the first composite Mongolians bow was invented in 1200 AD. The bows were made by combining of wood, bone, and glue taken from animal, and they were pressed and wrapped with birch bark. Because of their significant strength and accuracy, Mongolian bows had led Genghis Khan to achieve the victories. Thus, at that time, these weapons became the most used powerful ones because of the composite materials [12].

The discovery of natural plastics and resin extruded from plants and animals was not enough to start the new era for composite materials. The first developed plastics such as phenolic resins, polystyrene, vinyl and polyester were produced in early 1990-s, but plastics without reinforcement are still not a perfect material to provide sufficient strength if used in structural applications. The need for strong and rigid materials has led to invent for the first time the glass fibers by Owens Corning in 1935. The combination of glass fibers and polymer creates a significant strong lightweight structure. The application of fiber reinforced polymer has seen the light from that time, reaching the incredible various applications till now [13].

Throughout the time, more durable composite materials were introduced, until the World War II, when advanced achievement occurred by real use of FRP materials. By 1945, Military application used more than 7 million pounds of glass fibers. In addition, it was observed that the composite materials are perfect selection to boats, leading to introduce the first composite boat hull in 1946. Moreover, the largest consumption of composite materials by 1960s was by the marine. The composite automotive body was manufactured and tested for the first time in 1947, until the 1970s, when the consumption of composite in automotive industries got over that of marine as the number one automotive market increased and lasted till today. Continuously, composite materials advanced in many engineering sectors until late 1970s and early 1980s, when they first used in infrastructure applications in Asia and Europe. During 1990s, in Aberfeldy, Scotland, a composites pedestrian bridge was built.

In the last two decades of previous century, composites were widely used to obtain good performance structure of spacecraft and military aircraft after were being used only as insulators and radar-domes relaying on their electromagnetic properties. Moreover, the composites are used to produce tools that protect human against impacts and fire. Using more environmental friendly deign such as natural fibers in introducing composite is also used [11–13].

The increasingly success of using composite materials in terms of quality and quantity can be recognized by the accessibility and reproducibility of the manufacturing technologies. The new design and production operations must be done according to the variable parameters that lead to the optimum design such as shape, strength, cost, durability, etc.

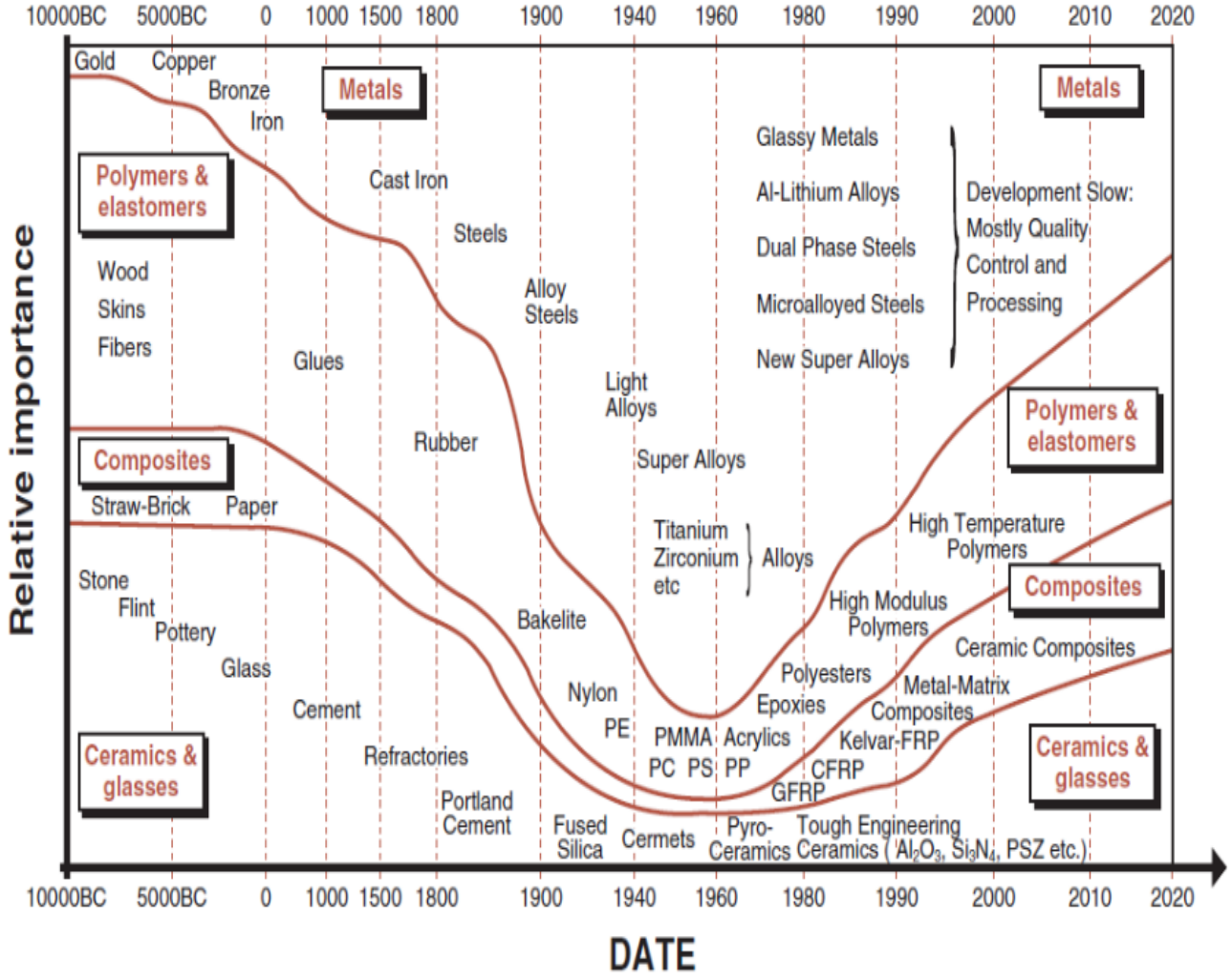

Figure 2. 1. Chronology of Structural Materials Developments [14].

2.2. *Concept of Composite Materials*

Composite material is a combination of materials (two or more) that are chemically distinct, insoluble, and different in properties. The objective aim of composite materials is to obtain performance properties that are superior to those of the constituents such as combining the flexibility and weight of a polymer with the strength of a ceramic in one material to have all properties.

In particular, composites consist of three components, the matrix as the continuous phase, the reinforcements as the discontinuous or phase, and the fine interphase region, also known as the interface [11].

Some examples of composite materials: (a) plywood is a laminar composite of layers of wood veneer, (b) fiberglass is a fiber reinforced composite containing stiff, strong

glass fibers in a softer polymer matrix , and (c) concrete is a particulate composite containing coarse sand or gravel in a cement matrix [15]

The advantages of the matrix are giving a bulky form to the composite product, holding the embedded materials, and distributing the load to the secondary phase so the reinforcement materials can bear the stress and the load can be shares [16].

The most used reinforcements in composites are continuous fibers, discontinuous fibers, whiskers, and particles. The reinforcement type chosen for a composite material is of great importance as it determines the outstanding properties of the finished part such as load-bearing ability, strength, impact resistance and specific stiffness.

A Fiber reinforced material has a much higher strength in fiber direction compared to the same material in other orientation, so continuous, aligned fibers are the most efficient reinforcement form and are mostly used in the applications that require high-performance. In order to achieve specific properties such as better impact resistance, continuous fiber might be converted into many types by using textile technology providing two- and three-dimensional fabrics and braids.

The unique combination of matrix and reinforcement depends on the interface structure to obtain the intended properties of the composite materials. The interface of reinforcement-matrix in composite materials determines its performance because some reinforcements are not compatible with the matrices in term of their physical and/or chemical properties leading to pre-operation failure of the composites.

The compatibility between fiber and matrix or the the fiber–matrix interface has been proved to be a factor that has primary impact on the overall mechanical properties of composite structures. Achieving the intended transferring of the stress from the matrix to the reinforcement is highly conditioned by having strong chemical and physical interfacial interaction between the matrix and the fiber. Weak interfacial contact because of inert surface fiber for example, is very likely to cause composite failure that based on interfacial debonding [17].

In Polymer composite for example, coupling of covalent bonds between polymer matrix and fiber is a strong desirable interaction. However, secondary forces such as Van der Waal forces or hydrogen bond can occur between the constituents.

To attain superior mechanical behaviour, the interfacial adhesion should be strong. The matrix molecules can be anchored to the fiber surface by chemical reaction (adsorption), which determines the extent of interfacial adhesion. The interface is also called as the mesophase [18].

The advantages of using composite materials in all sector of application can be summarized by the following:

- High specific strength.
- High specific stiffness, long fatigue life.
- High creep resistance.
- Low coefficient of thermal expansion.
- Low density.
- Low thermal conductivity.
- Better wear resistance.
- Improved corrosion resistance.
- Better temperature dependent behaviour.

Although that the great importance of composite materials, there are limitations of using them. These limitations can be summarized by the following:

- Properties of many important composites are anisotropic - the properties differ depending on the direction in which they are measured – this may be an advantage or a disadvantage
- Many of the polymer-based composites are subject to attack by chemicals or solvents, just as the polymers themselves are susceptible to attack
- Composite materials are generally expensive
- Manufacturing methods for shaping composite materials are often slow and costly.

2.3. *Classification of Composite Materials*

Based on their material phases, composites can be classified into more than one distinct way. For example, regarding the material of the matrix, the composite materials can be classified into the following:

- Polymer Matrix Composite, PMCs
- Metal Matrix Composite, MMCs
- Ceramic Matrix Composite, CMCs
- Carbon / Carbon Composite, C/Cs

Regarding the reinforcement phase, composite materials can also be classified as:

- Fiber Reinforced Composites (continuous/ short)
- Particulate Reinforced Composites
- Whisker Reinforced Composites
- Flakes Reinforced Composites
- Structural Composites (Laminated / Sandwich)

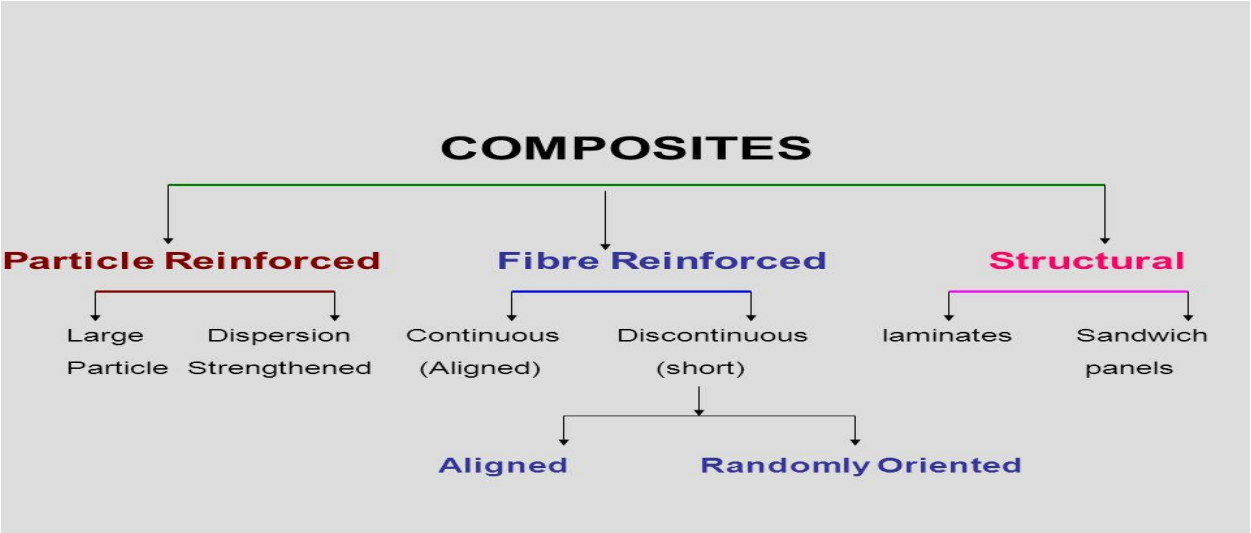

Figure 2. 2. Classification of Composite According to the Reinforcement

2.3.1. Polymer Matrix Composites (PMCs)

They are the dominant type of composites that used nowadays in most of the commercial applications. The main advantages of polymers as matrix are easy process-

ability, low cost, good chemical resistance, and low specific gravity. However, there are other properties that limit its use such as low strength, low modulus, and low operating temperatures. The Reinforcement of polymers by strong fibrous network leads to the development of PMCs, which is characterized by higher level of properties that make the PMCs are as beneficial materials as they are nowadays [19].

2.3.2. The Reinforcement of PMCs

The high strength and stiffness of advanced PMCs are obtained by the continuous fiber reinforcing. Glass, graphite, and aramid are the dominant types that are currently used in this class of composite materials based on their mechanical and physical properties. Glass fiber reinforced plastics (GFRPs) have shown the structural and durability demands in all types of interior and exterior applications. Good mechanical properties have led to the entry of GFRPs in the automotive industry. however they exhibit some disadvantages such as their relatively high fiber density, difficulty in machining, and poor recycling property [20].
During the past decade, the chance of using natural fibers as reinforcement for thermoplastic and thermoset matrices has been explored as they have been successfully utilized by automobile manufacturers and suppliers for door panels, seat backs, headliners, package trays, dashboards, and interior parts. Recently, Natural fibers have also attracted the attention of researchers, engineers and scientists as an alternative reinforcement material for fiber reinforced polymer (FRP) composites [3, 19].

2.3.3. Properties of Polymer Composite Materials

- High specific strength.
- High specific stiffness.
- High fracture resistance.
- Good abrasion resistance.
- Good impact resistance.
- Good corrosion resistance.
- Good fatigue resistance.
- Low cost

2.3.4. Factors Affecting Properties of Polymer Matrix Composites

- **Interfacial Adhesion:** The characteristics of PMCs are obtained based on the combined characteristics of the reinforcing material, polymer matrix, and the fiber-matrix interface. To attain superior mechanical behaviour, the interfacial adhesion should be strong. The matrix molecules can be anchored to the fiber surface by chemical or physical reaction, which determines the extent of interfacial adhesion. The interface is also called as the mesophase. The strongest anchoring of the matrix is achieved by the chemical reactions such as the amine functionalized carbon nanotubes in epoxy resin [21].
- **Shape and Orientation of Dispersed Phase Inclusions (Particles, Flakes, Fibers, and Laminates):** Particles are mainly used to improve properties or lower the cost of isotropic materials and they do not have preferred directions. Their shape can be spherical, cubic, platelet, or regular or irregular geometry. The dimensions of the particulate reinforcements are

approximately equal in all directions. Large particle and dispersion-strengthened composites are the two subclasses of particle reinforced composites. The laminar composite is composed of two sheets or panels. The layers are stacked together so that the orientation of the high strength direction varies with each successive layer [19].

2.3.5. Applications of PMCs

- Aerospace structures: The military, commercial airlines, Space shuttle, satellite systems.
- Marine: Boat bodies, canoes, kayaks, and so on.
- Automotive: Body panels, leaf springs, drive shaft, bumpers, doors, racing car bodies, and so on.
- Sports goods: Golf clubs, skis, fishing rods, tennis rackets, and so on.
- Biomedical applications: Medical implants, orthopaedic devices, X-ray tables.
- Electrical: Panels, housing, switchgear, insulators, and connectors.
- Chemical storage tanks, pressure vessels, piping, pump body, valves, and so on.

2.3.6. Polymer Matrix Composite Classifications

This type of matrix material composites can be classified into two groups (thermoplastic and thermoset). Each type has it is own characteristics as shown below [5]:

Thermoplastic
Thermoplastics consist of linear or branched chain molecules having weak intermolecular bonds. They can be reshaped by application of heat and pressure and are either semi crystalline or amorphous in structure. Examples include polyethylene, polypropylene, polystyrene, nylons, polycarbonate, polyacetals, polyamide-imides, polyether ether ketone, polysulfide, polyphenylene sulphide, polyether imide, and so on.

Thermoset
Thermosets have cross-linked or network structures with covalent bonds with all molecules. They do not soften but decompose on heating. Once solidified by cross-linking process they cannot be reshaped. Common examples are epoxies, polyesters, phenolics, aminoplasts, ureas, melamine, silicone, and polyimides .

Table 2. 1. Properties of Some Polymer Matrix Materials [15, 19].

Matrix	**Materials**	**Density (g/cm^3)**	**Tensile Strength (MPa)**	**Tensile Modulus (GPa)**
Thermoplastics	Polyethylene	0.90-0.98	25-35	0.4-1.1
	Polypropylene	0.90-0.94	28-40	0.5-1.3
	Polycarbonates	1.20-1.22	65	2-3
	Polyamides	1.13-1.41	78	2.6-3

	Polyphenlyne Sulphide	1.34	90-95	3.4-3.6
	Polyethermide	1.27	40	5-5.5
	Polyether ether ketone (PEEK)	1.26-1.32	95-220	4-20
Thermosets	Phenolic	1.1-1.40	45-50	3.5-3.9
	Epoxy	1.1-1.70	50-70	2.3-2.5
	Bismaleimides	1.15-1.36	70-80	25-28
	Cyanate Esters	1.18-1.30	50-90	2.6-3.1
	Polyimides	1.42-1.85	90-120	n.d

2.3.7. Processing of PMCs

There are different methods for fabricating PMCs. Generally, all of the methods involve the following basic steps [22, 23]:

- Impregnation of the fiber with the resin,
- Forming of the structure,
- Curing (thermoset matrices) or thermal processing (thermoplastic matrices), and
- Finishing.

Below are the commonly used techniques of fabricating PMCs.:

- Spray Lay-up Method
- Wet lay-up, Hand lay-up Method
- Vacuum Bagging Method
- Filament Winding Method
- Pultrusion Method
- Resin Transfer Molding (RTM)
- Compression Molding Method
- Injection Molding Method

3. DAMAGES OF COMPOSITE MATERIALS

3.1. *Introduction*

Although of the attractive properties of composite materials mentioned earlier, there are critical issues that may limit their usage. The most revealed aspect of these issues is the damages of composite materials. Damages may arise in composite materials, putting the structure in a risk. Due to the heterogynous microstructure of the materials and big difference of the constituent's properties, the mechanism of the damage is clear Also, the interface presence and the fiber orientations give anisotropy in overall properties of the materials.

The mechanism of damages in composite materials is not easily predicted and understood due to the nature of the material. Defects and fracture generally may occur during the manufacturing process or service life of the structure or parts. The damage mechanisms in a fibrous composite are broadly categorized as:

A- Micro-level damage: This can be classified into fiber level damage and matrix level damage mechanisms. Regarding both levels, many damages can occur such as fiber breaking, fiber buckling, fiber bending, fiber splitting, and matrix cracking.

B- Macro-level damage: The macro-level mechanisms are laminate level mechanisms. It is seen that the adjacent layers are bonded together by a thin layer of resin between them. This interface layer transfers the displacement and force from one layer to another layer. When this interface layer weakens or damages completely, it causes the adjacent layers to separate. This mode of failure is called delamination.

C- Coupled Micro-Macro Level Failure Mechanisms: The through thickness transverse crack may propagate to neighbouring lamina causing it to break [15].

In other words, depending on the stress applies to the composite part and the reinforcement type of the composite itself; there are basic stages of the damage process. The damages that occur in the beginning require low energy consumption, such as damages of the matrix phase and of interface. Furthermore, the later occurring damages or deeper damages such as fiber breakage require higher amount of energy consumption [24].

The zone of lower strength in the composite parts such the matrix or the interface is the area of the first step of damage causing failure of that could also called the **intralaminar** cracks as shown in figure 3.2. In this type of crack, the strain reaches its maximum value of breaking, usually causing parallel and spaced defects. The damages caused by this type usually occur in the area where the fiber orientation is not parallel to the loading axis. Their impact on the overall material strength are little [7].

Moreover, there is a damage called **interlaminar** when the cracks appear in a ply of laminated composites. In this failure, the stresses of the intralaminar cracks lead to the

cracks to propagate at the interface of the adjacent layers caused delamination, see figure 3.2. The source of delamination could be manufacturing flaws of any other impacts.

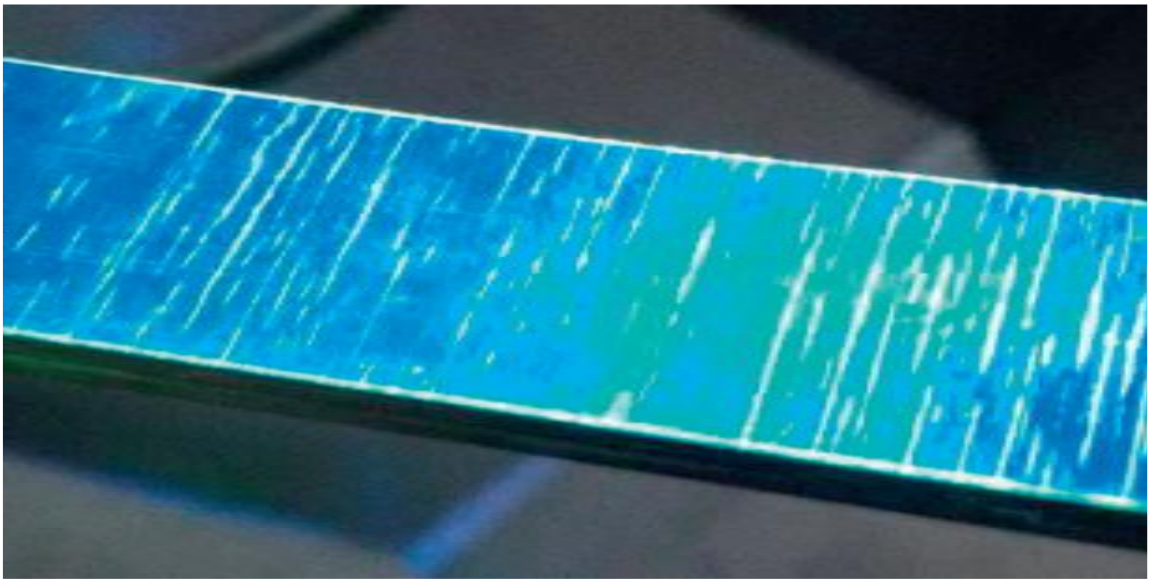

Figure 3. 1. Intralaminar Cracks [7].

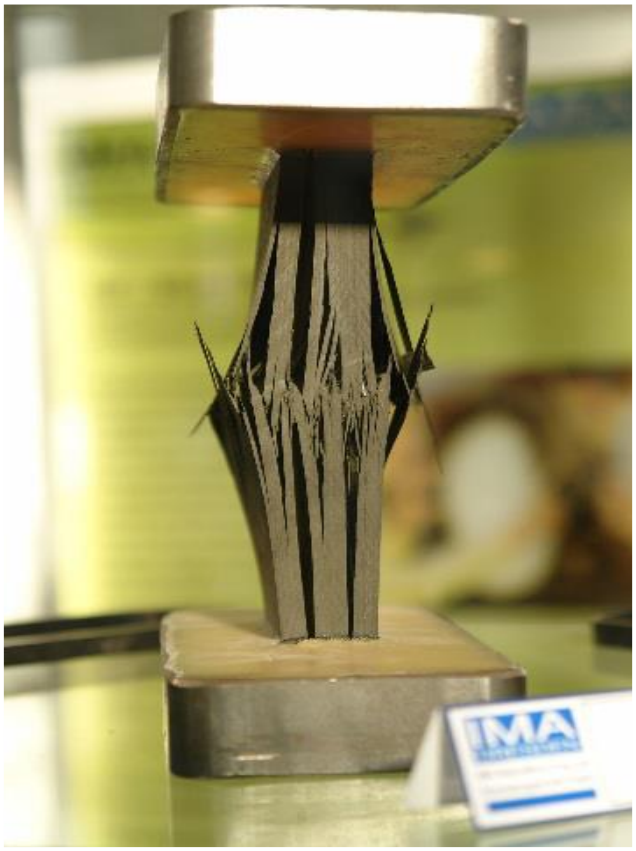

Figure 3. 2. Delamination [9].

The damage size of the matrix may go through the thickness reaching certain level that cause the lamina to break resulting from the fiber breaking. This is the **translaminar** failure which is the last stage of the composite part deterioration which occurs at the zone of high-applied load, figure 3.3.

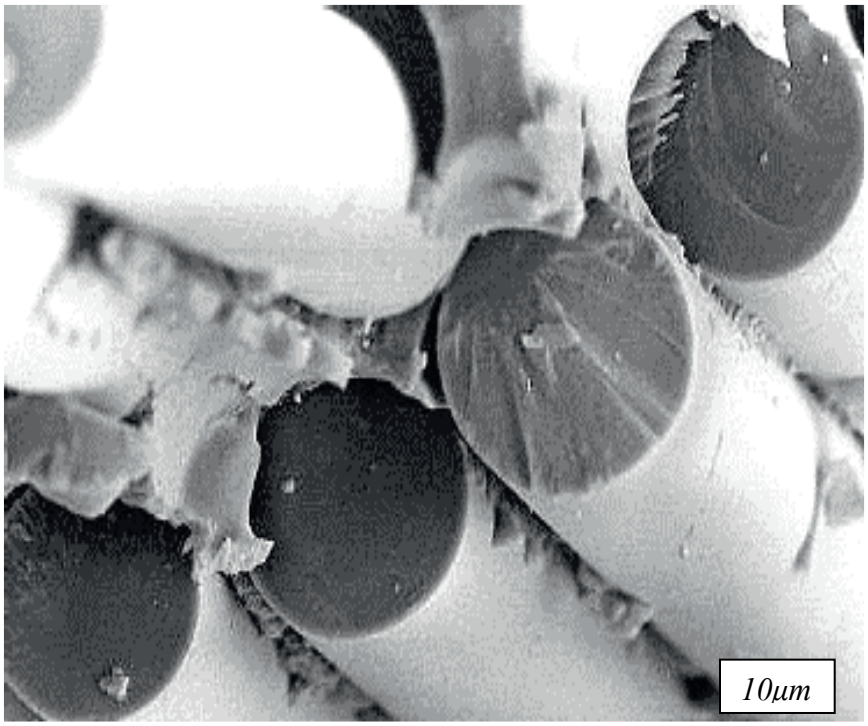

Figure 3. 3. Translaminar Failure[7].

As mentioned above, the damages of composite materials can also be grouped based on the occurrence occasion. For example, there are defects or damages that occur during the manufacturing process which includes material processing and part manufacturing. The other occasion of damages occurring is during service life damages. Below are brief description of the three occurrence occasions [10]:

- Material Processing: This process includes the production and preparation of the constituents of the composite materials of a prepreg such as the process of pre-impregnated composite fibers. The defects in this stage might occur because of improper storage or quality control and batch certification procedures leading to material variations.
- Component or part manufacture: it is the process of making the composite part or component according to previous required need or design. Damages in this stage induced defects occur during either the layup and cure or the machining and assembly of the components.
- In-service Period. This stage is where the composite structure faces all the risks of operation time. Damages here might be a result of environmental or mechanical actions. In service damages occur because of impact and handling, overloading, heating, chemical attack, ultraviolet radiation, fatigue, or other reason.

Table 3. 1. Damages During the Processing, Manufacturing Process or Service Life [10].

Material Processing Damages	**Component Manufacturing Damages**	**In service Damages**
Fiber distribution variance	Contamination	Corner/edge crack
Fiber faults	Corner/edge splitting	Corner radius delamination
Fiber/matrix debond	Cracks	Creep
Fiber misalignment	Delamination	Delamination
Miscollination	Debond	Debond
Over-aged prepreg	Excessive ply overlap	Erosion
Prepreg variability	Fastener holes	Fiber kinks
	Fiber kinks	Fracture
	Fiber misalignment	Matrix cracking
	Fracture	Matrix crazing
	Voids	Surface damage
	Porosity	Surface oxidation
	Missing plies	Surface swelling
	Variation in density	Translaminar cracks
	Warping	Fiber buckling
	ply waviness	
	inclusions such as dust or pre-preg backing paper	

Since the manufacture of composite materials is a delicate process, special care must be taken. However, damages occur even though the great care that has been given during the process. According to some studies manufacturing defects has noticeable effects of the mechanical properties of the composite parts [25–27].

Table 3. 2. Few Types of Manufacturing Defects with Their Effects of the Mechanical Properties.

Defects type	**Mechanical Property**	**Effects**
Fiber waviness	Tensile modulus	No loss
	Tensile strength	20% loss
	Poisson's ratio	100% increase
10 % voiding	Compressive strength	15 % loss
	Interlaminar shear strength (ILSS)	30 % loss
	Interlaminar shear modulus	30 % loss
Paper inclusion	ILSS	25 % loss
	Compressive strength	20 % loss
Cut fiber tow	Tensile strength	25 % loss
	Compressive strength	11 % loss

3.2. *Brief Description of the Most Frequent Occurring Damages*

3.2.1. Matrix Cracking

It is a very common mode of failure that mostly occurs in polymer matrix composites. This type of damage could be generated because of the overloading of various operation conditions. The crack could occur at low level of load consumption low fracture energy varying based on the epoxy composites (lower energy) or the thermoplastic composites (higher energy). In most cases, the matrix crack is measured to be localized damage and sometime hard to detect. However, under certain conditions such as fatigue loading, it leads to delamination.

3.2.2. Delamination

It is one of the most frequently occurring types of damage in long fiber composite materials. When the matrix crack propagates within the interface of plies in the laminate and when it is parallel to fiber orientation, delamination occurs by separating the plies and result in significant reduction in compression and shear strength of the structure. In fact, the compression strength of composite part is at a risk of being reduced to 50 percent by small areas of delamination [25].
Delamination mostly occur because of an impact or un accurate manufacturing and it may initiate and propagate under static or cyclic tensile loading [28]. It was stated that the delamination is at the most sever level if the relative angle between the separated plies is the greatest [29]. Based on the matrix material, the energy consumption in the delamination fracture differs between 100 J/m^2 in epoxy based composite and 300 J/m^2 in thermoplastic based composites [25].

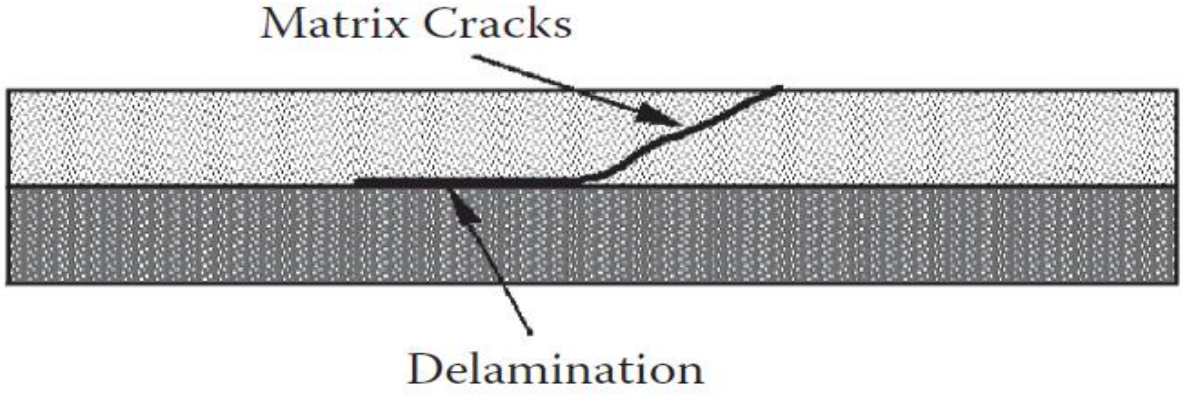

Figure 3. 4. Matrix Crack and Delamination initiation[10].

3.2.3. Fiber-matrix deboning

It affects the interface by separation of the matrix and the fiber. The interface debonding happens if the applied stress exceeds the local strength. It is not easily predicted by vision or by conventional detection methods because it is a localized failure mode. The resulted debonding amount basically depends on the quality of surface treatment of the fibers during the fabrication of the pre-preg. Low level of

surface treatment usually make the fiber suitable to easier debonding resulting in rough fracture surface with three dimensional view when using a scanning electron microscope (SEM), while highly treated fibers tendency to debonding is less and the fracture is planar with the crack propagation across the fiber [25].

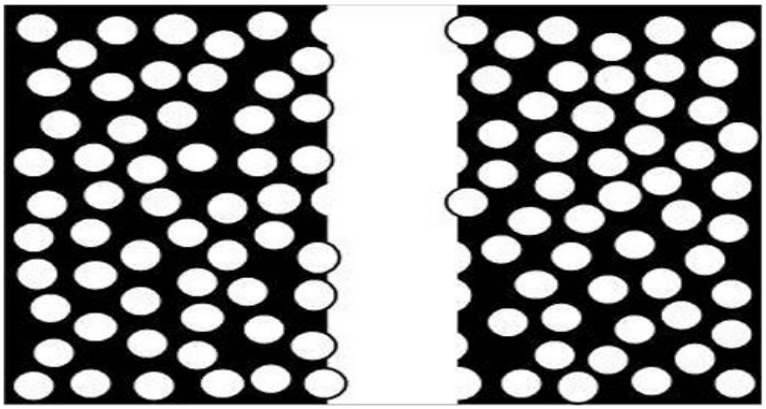

Figure 3. 5. Fiber-Matrix Debonding [10].

3.2.4. Fiber Fracture

This type of damage has significant effect on the stiffness and strength particularly tensile strength of fiber reinforced composites because the fiber is the most load-bearing constituent in this kind of materials. There were many investigations suggesting that failure of composite components can occur by fracturing of even small number of fibers [25, 28].
The reason behind fiber fracture could be:

- Transverse impact loading which often creates immediate zones of localized fiber fracture in the point of impact.
- Compression fatigue cycling also has been proven to generate of large, angled cracks in the 0-degree fibers in a (0 degrees ± 45 degrees) laminate.

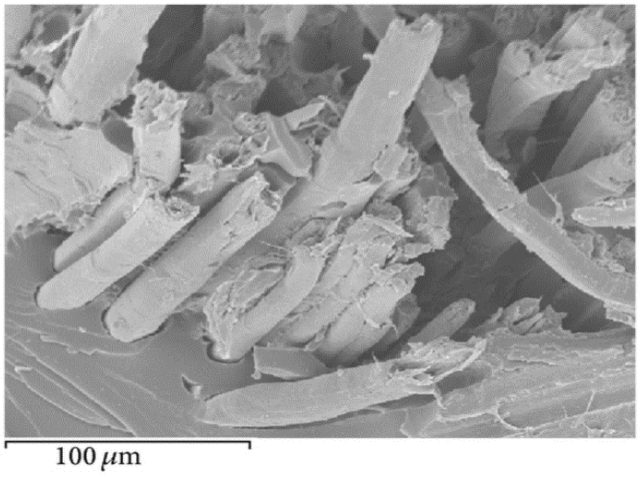

Figure 3. 6. Fiber Fracture [9].

3.3. *Fatigue In Composite Materials*

Significant number of the working conditions of mechanical parts includes cyclic loading. This brings the risk of fatigue failure of the part even within the limits of loading amounts that is below the elastic limits of the materials. Thus, optimising the design and obtaining the reliability that ensure a safe service life, require a knowledge of the fatigue behaviour and the mechanical properties of the composite materials.

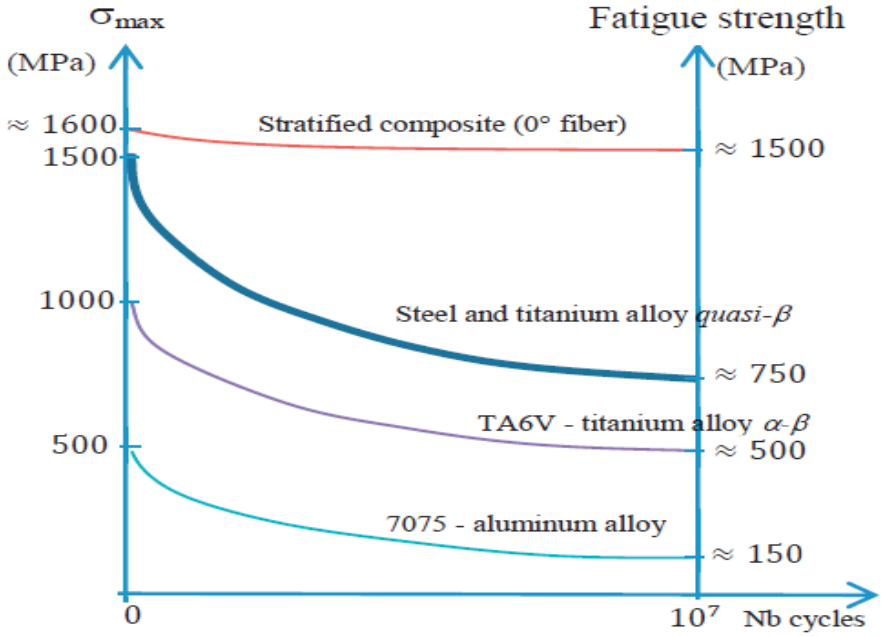

Figure 3. 7. Fatigue Strength for Different Materials Including Composite [7].

Although that the fatigue analysis and calculations tools of metals are not appropriate for that of composites, many calculations have presented that fatigue strength in tension for composite materials is superior to metallic material such as titanium alloy or aluminium alloy. Also, it was verified that the fatigue does not act as an obstacle in the composite use, nor assistant to the propagation of composite damages [7, 30].

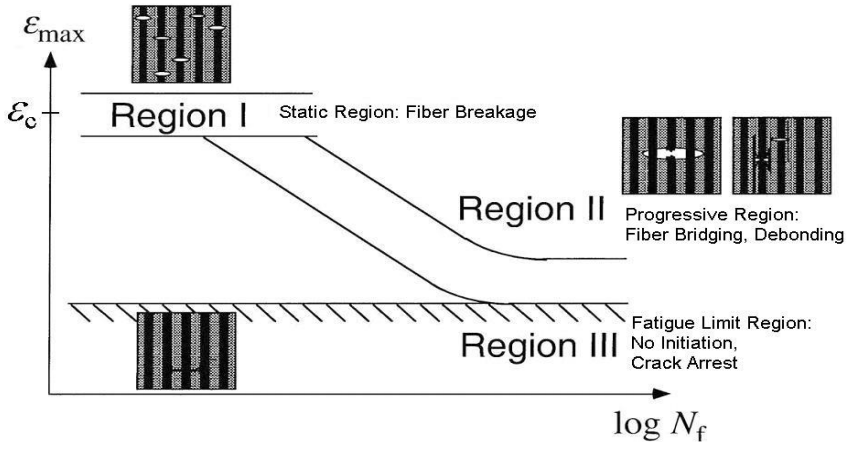

Figure 3. 8. Schematic Illustration of Fatigue Life Diagram for a Unidirectional Composite, Showing Three Regions with Different Damage Mechanisms [31] .

According to Talreja (1981) that the fatigue life diagram resulted data can be classified into three regions. The first region (region I) is called the static region in which the fiber failure is not progressive. It appears as a horizontal scatter in the diagram.

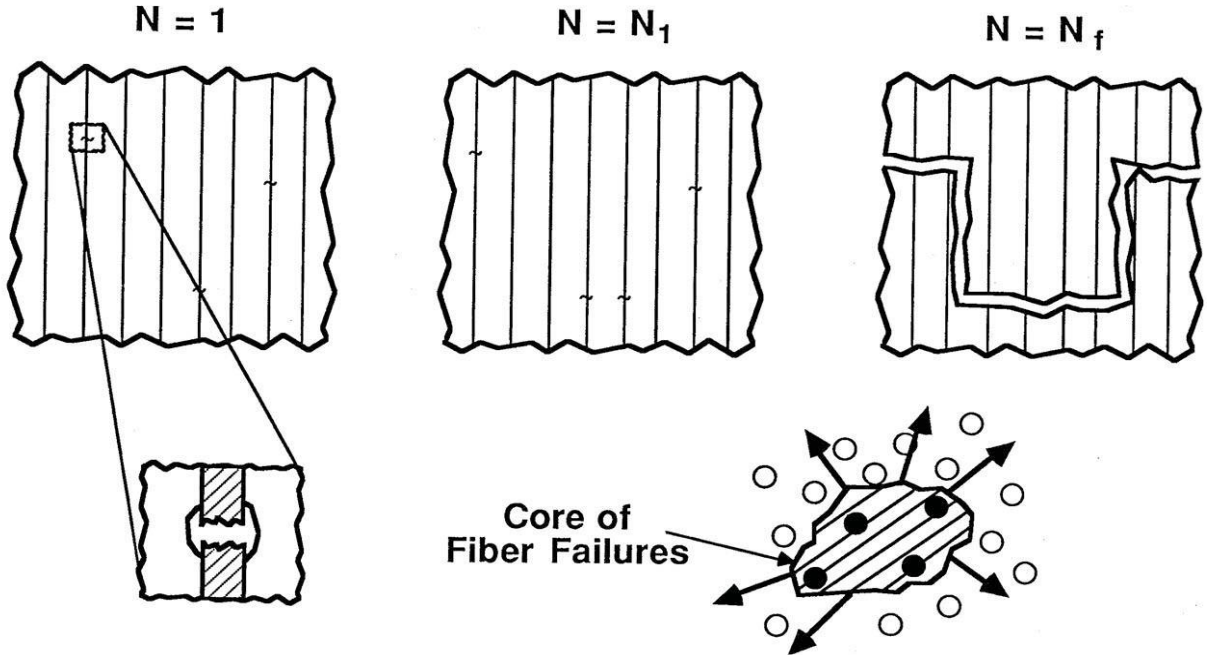

Figure 3. 9. Static Fiber Breakage in Region I [31].

At a certain number of the cyclic load, region II is deviating from region I and extending down to the fatigue limit. In region II, a progressive crack mechanism occurs when a fiber-bridged matrix crack happens.

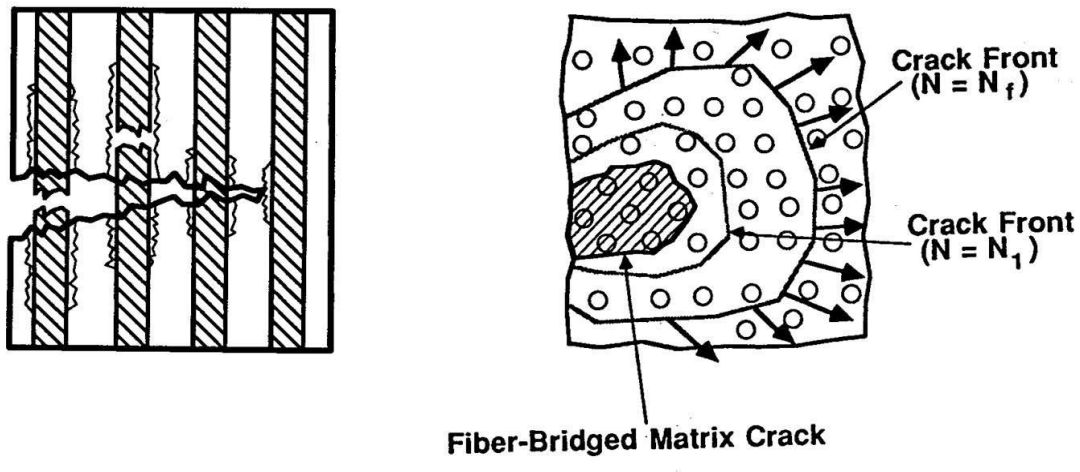

Figure 3. 10. Fiber Bridged Matrix Cracking in Region II [31].

Region III is the final region of the fatigue life diagram which lies below the fatigue limit, where no fatigue failure occurs.

4. DAMAGE DETECTION METHODS IN COMPOSITE MATERIALS

4.1. *Introduction*

In order to have an early prediction of existence of visible or non-visible damages in composite structure and avoid failure, many structural health monitoring (SHM) methods have been revealed. Among these methods is what is known as non-destructive inspection (NDI) methods. These methods are used in different ways to indicate the damage location and evaluate the damage in term of size, type, and shape. Moreover, the information gathered from these methods help in post-repair quality insurance [10].

Visual examination is simply the initial basic way of damage assessment. It provides the inspector with simple information like the location of the damaged area and the severity of the damage. After that, following the extent and the range of damages require more sensitive non-destructive methods. When dealing with defects of composite materials and structures, information and details provided by the NDI method are of great importance because of the complexity and the anisotropy of the materials. The damage might be hidden with barely visible or no dent on the surface requiring and accurate inspection methods [25].

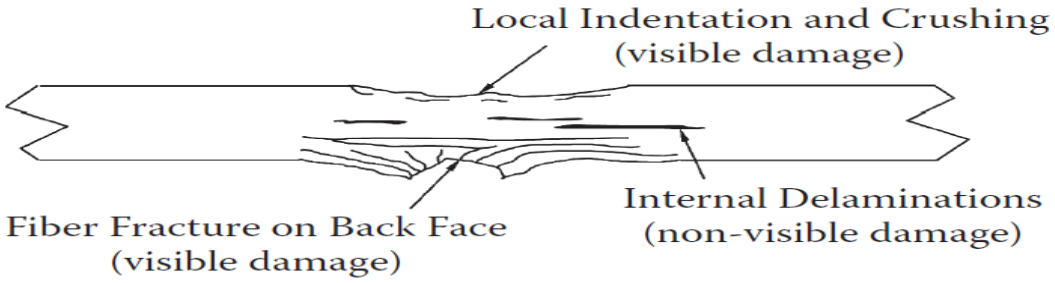

Figure 4. 1. Internally Hidden Damage with External Visible Damage [10].

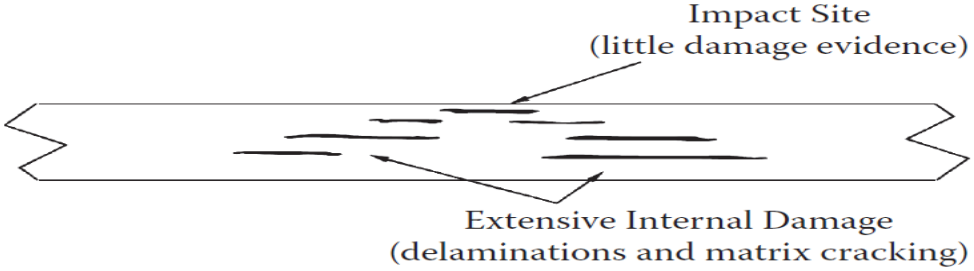

Figure 4. 2. Barely Visible Impact Damage [10].

4.2. *Ultrasonic Inspection Technique*

It is one of the most conventional methods that used to inspect damages in composite materials (particularly laminated composites). It involves placing a transducer at the composited panel to assess its quality. Two principal methods of the ultrasonic techniques are used based on the transducer placement. A-Scan methods (Pulse echo) which involves using same transducer that emitted the original pulse, or C-Scan which involves placing a transducer at the rear of the panel through transmission [25].

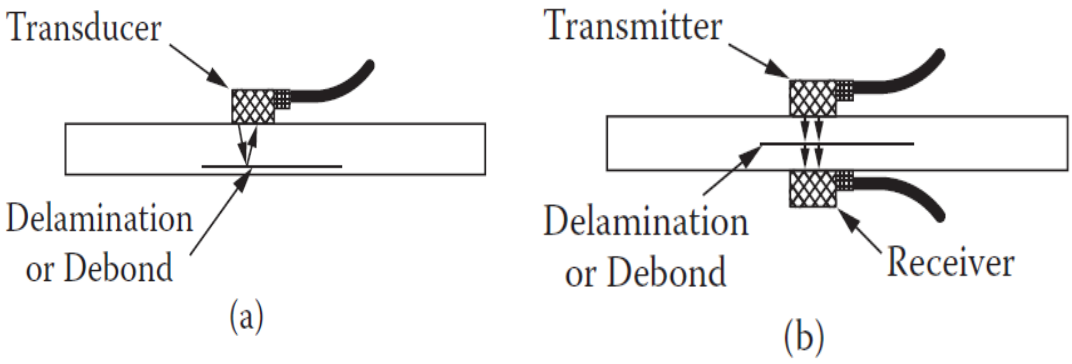

Figure 4. 3. Ultrasonic Inspection Techniques, a- A-Scan, b- C-Scan [10].

Both methods involve directing ultrasonic signal towards the component of interest. In other words, as the sound pass through the area of interest, it measures the change in the sound attenuation or the amplitude loss. the process involves immersing he test probe in water or coating it with grease, or transmitting the signal through jet of water, in order to maintain maximum transmission of the ultrasonic energy [32].

4.3. *Thermography*

This NDI technique stands upon measuring the response to the dissipation thermal energy and temperature induced through the defected composite part. There are two analysis types involved in this inspection method, namely active and passive thermography techniques. The passive analysis determines the internal damages when observing that the rate of thermal energy dissipation is reduced, which can be observed by infrared sensitive camera. The active one is relied on vibration or load cycling the specimen, and in case of damage, the increased localized stresses generate heat. Generally, the thermography methods require experienced inspector and standards to verify the results [33].

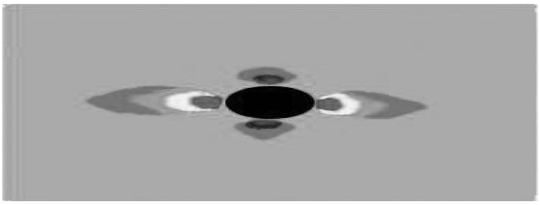

Figure 4. 4. Schematic of Thermography Results [10].

4.4. *Modal Analysis*

The experimental modal analysis is a technique that has been used to study dynamic characteristics of mechanical components. Furthermore, in recent years the modal analysis has been used to measure the performance and efficiency loss of working structures because of eventual degradation of individual components. The progression of such factors leads gradually to change the material performance resulting in changes the variation characteristics. The characteristics meant in such cases are modal frequencies, mode shapes and damping properties of structural components. These parameters can be delivered by modal analysis testing. the experimental modal analysis are proven to be able to test in site structures and with even large scales [34].
There are two methods used for the excitation of the structure for modal measurements. Namely, these two methods are the input-output (active excitation) and output only (operational excitation). In the Input-output methods of excitation, the procedure involved consists of an ex-citing function introduced to initiate vibration of the structure. Typically, the forms of excitation entail are impact hammers, drop weights, shakers, or displacement-release. The waveforms used in modal analysis can be of various natures, including harmonic and random input, as well as impulsive excitation. In the Output only method, excitation is present if the structure is in service and under some form of external excitation, e.g., traffic or wind loads. In field testing, dynamic properties are extracted by placing several motion sensors (commonly accelerometers) at predetermined locations along the structure. To suit the need for full-motion recording, triaxial accelerometers are commonly given preference. The objective of placing sensors in multiple locations is to attain a sufficient amount of frequency response functions (FRF), such that individual modes can be identified from the modal test. Herein, the highest measurable mode de-pends largely on the optimal placement of accelerometers; i.e., the extraction of higher modes demands a higher number of accelerometers.

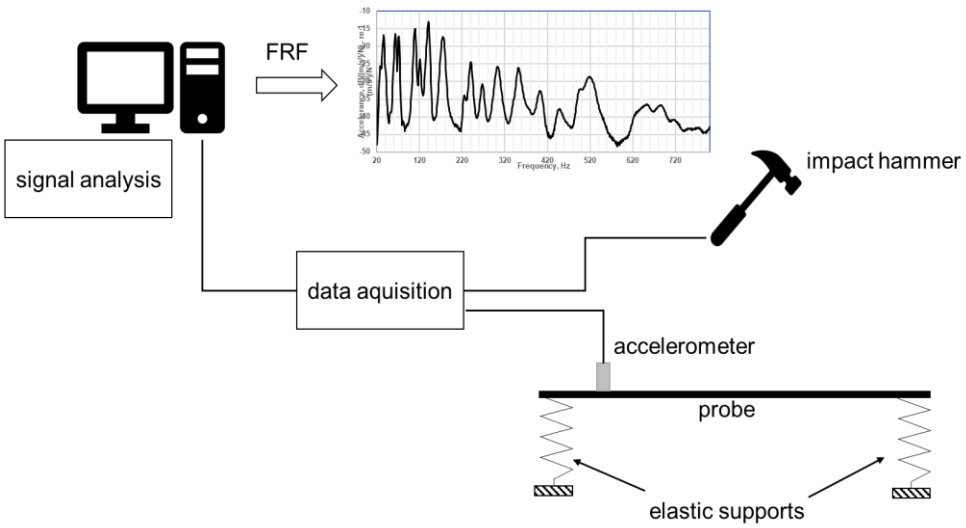

Figure 4. 5. Schematic Representation of Modal Analysis test.

4.5. *Radiography*

There are two main methods of the radiography technique, X-ray and neutron radiography. Generally, the method depends on the absorption differentiation of the radiation by the examined component.

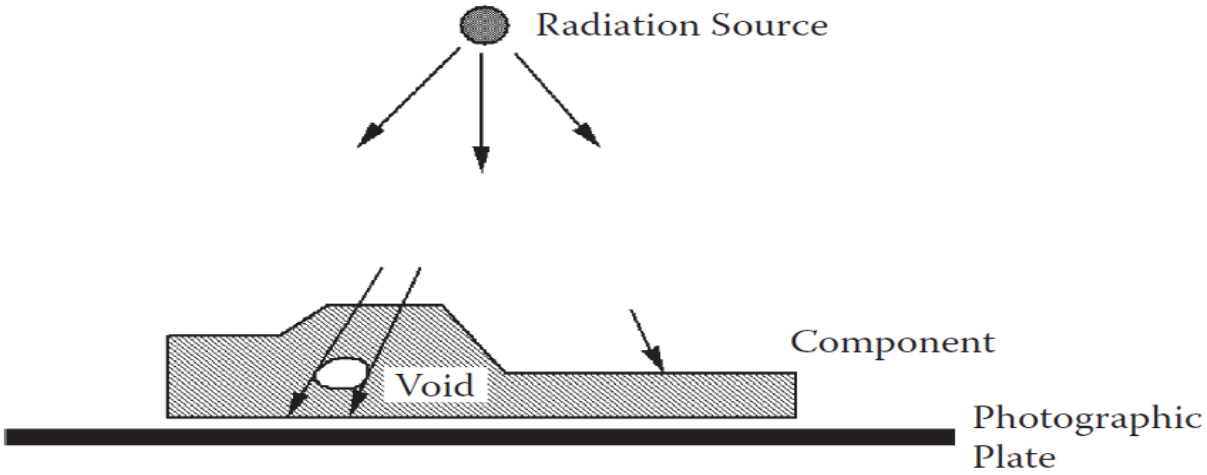

Figure 4. 6. Schematic of Radiography Principle [10].

The X-ray type requires experienced operator and expensive equipment and it is the perfect choice for the honeycomb sandwich panel inspection. It provides a permanent record and can be enhanced with dye penetrants. The Neutron radiography provides higher resolution of results but it is very costly [10].

4.6. *Guided Waves*

Guided wave-based technique is one of the most conventional non-destructive methods that used in damage investigation of composite materials. These methods are popular because of its ability to detect small size damages as well as the large detection area and the low attenuation. However, theoretical simulation of guided wave propagation in large composite structures may create in some cases a complex finite element models that would be hard or impossible to solve and analyse [35].
There are many methods of the guided wave-based techniques such as lamb waves, wave field imaging, Rapid methods and others. Lamb-waves are the most popular one among them. They are an elastic wave that their particle movement is directed by two parallel planes. There is a well-recognized property of the lamb wave which is its reflection and scattering from damages of the parts giving this method the ability to localize defects in the structures. The Lamb waves interact with delamination in a way that causes mode conversion in both sub-laminates at the start and end of the delamination region. As it is proved that the delamination causes a stiffness reduction in the affected areas, many researchers found that the velocities of lamb waves movement in the delamination area are different from those of undamaged components [36].

4.7. *Vibration Decay Rate*

It is one of the method that customized by the author to be used as a technique for composite material damages inspection [37]. Generally, there are several methods for the experimental determination of the damping of materials. One of these methods is the determination of the decay rate, which gives a relatively simple method for the loss factor determination [38]. The measurement of vibration decay rate is pretty like the measurement of the acoustic decay rate, which is well known in the room acoustics. The only difference is the usage of vibration sensor, e.g., accelerometer instead of microphones.
The probe whose decay rate is determined, must be excited with a mechanical impulse (e.g., impact hammer) or with a burst random signal (electro-dynamic shaker) and the time signal of the accelerometer on the structure is measured (impulse response). After the stop of the excitation the gradual drop of the acceleration level within a certain time can be observed in the signal. The length of this time is depending on the internal damping of the material [39]. Additional effect, e.g., the noise radiation can act like a damping, but this phenomenon is neglected in this investigation.
The drop of the energy level by 10^6 (or by 60 dB) in the measured time is called in the acoustics the reverberation time (RT60). The Reverberation Time (RT60) is the time that the sound pressure level takes to decrease by 60 dB after a sound source is abruptly switched off.
The RT60 decay rate must be filtered and the envelope should be created (e.g., by Schröder integration) in order to get the decay rates for every third octave frequency band. The Schröder integration is necessary to avoid the random error in the decay rate curves. The filtered T60 is considered for the further calculation of the loss factor over the frequency by the following formula [40]:

$$\eta = \frac{2{,}2}{f \cdot T_{60}}$$

f: is the mid frequency of a third octave band in Hz,
T_{60}: is the decay rate for each third octave mid frequency in s.
Value of 2,2: can be derived from the energy drop to the one millionth of the initial value.

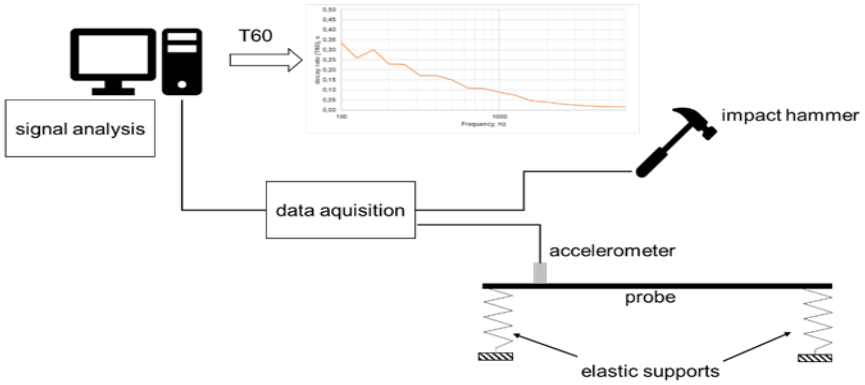

Figure 4. 7. Schematic Representation of Vibration Decay Rate Test.

4.8. *Acoustic Emission (AE)*

Acoustic emission technique is a non-destructive test that has been proved to have significant importance in inspecting the composite materials. As the component is under stress and undergoes defects and deformation, there will be a transient elastic stress waves generated as a result, so the technique includes the generation, propagation and then detection of the resulted stress waves [41].
Typically, there will be a transducer that detects the stress waves that propagate to the surface of the material. It is worthy to mention that the ability of the sensors (transducer) to detect the surface displacement of the investigated part is a condition to make use of the acoustic emission technique. The transducers or sensors are most commonly made of a piezoelectric material which are suited to be able to convert the surface displacement resulted from the acoustic waves into a signal which then can be recorded and stored for further analysis. Transducers are directly connected to the measured surface with the help of special gluey or adhesive material that can enhance the vibration transmission from the structure to the transducer.
Generally, the acoustic events are developed by applying a load from an active source. The source is an active damage, flaw, or nonconformity in the material. The term active belongs to the fact that at the given load, the flaw or damage is generated and progressed. This could be considered as a major drawback of using AE technique when compared to others that could detect passive damages. In spite of the ability of AE technique to detect almost all the failure modes of the composite which involve (matrix cracking, fiber/matrix debonding, fiber pull-out, fiber fracture, and ply delamination), it is not easy to distinguish among them which could be another disadvantage of the AE method. Other limitations of using AE methods could be:

- Tendency of composite materials to attenuate and disperse of propagating stress waves which may require using several transducers on large or complex structures.
- Requires experienced operators to set up the system and interpret the results because it has complex output to be understood and analysed.
- The condition of applied loading is not always reproducible.
- There is a need of extensive pre-amplification because the energy of the AE events is relatively very small.
- Always requires a filtering off the background noise which is not an easy task.

However, there are noticeable advantages of using AE technique for composite materials inspection. Below are some of them:

- The deep analysed output of the AE technique can locate the “flaw” over the entire surface of parts and structures without a point-by-point scanning as some other non-destructive tests (NDTs) require.
- The AE technique is reasonably sensitive to small changes in defects.
- It is portable and recordable.
- The online monitoring which means a real-time continuous monitoring of the “nonconformity” also while structures in service.

During the monitoring process of the AE, there is a challenging step includes how to determine whether it is transient (burst) signal or continuous signal. As it is stated that the continuous type of AE signal is belonging to friction phenomena with in the

damaged region, it is usually disregarded in the signal processing. Thus, the investigations and studies of AE focus on the burst type one because they are linked with development of flaws in the composite parts [10, 25, 41].

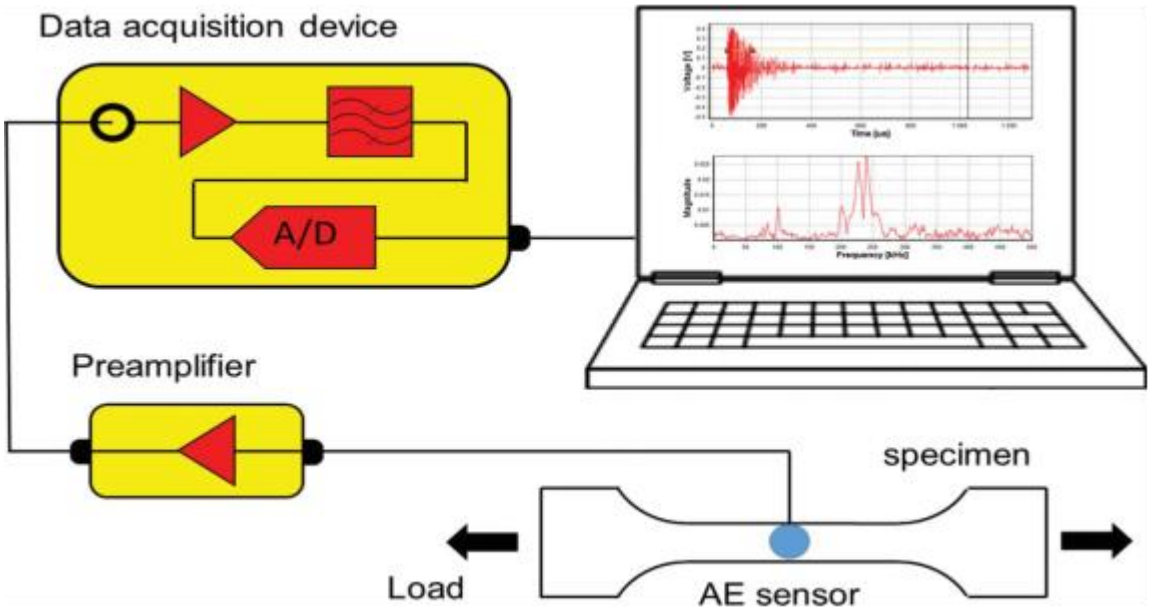

Figure 4. 8. Schematic Representation of AE Test [41].

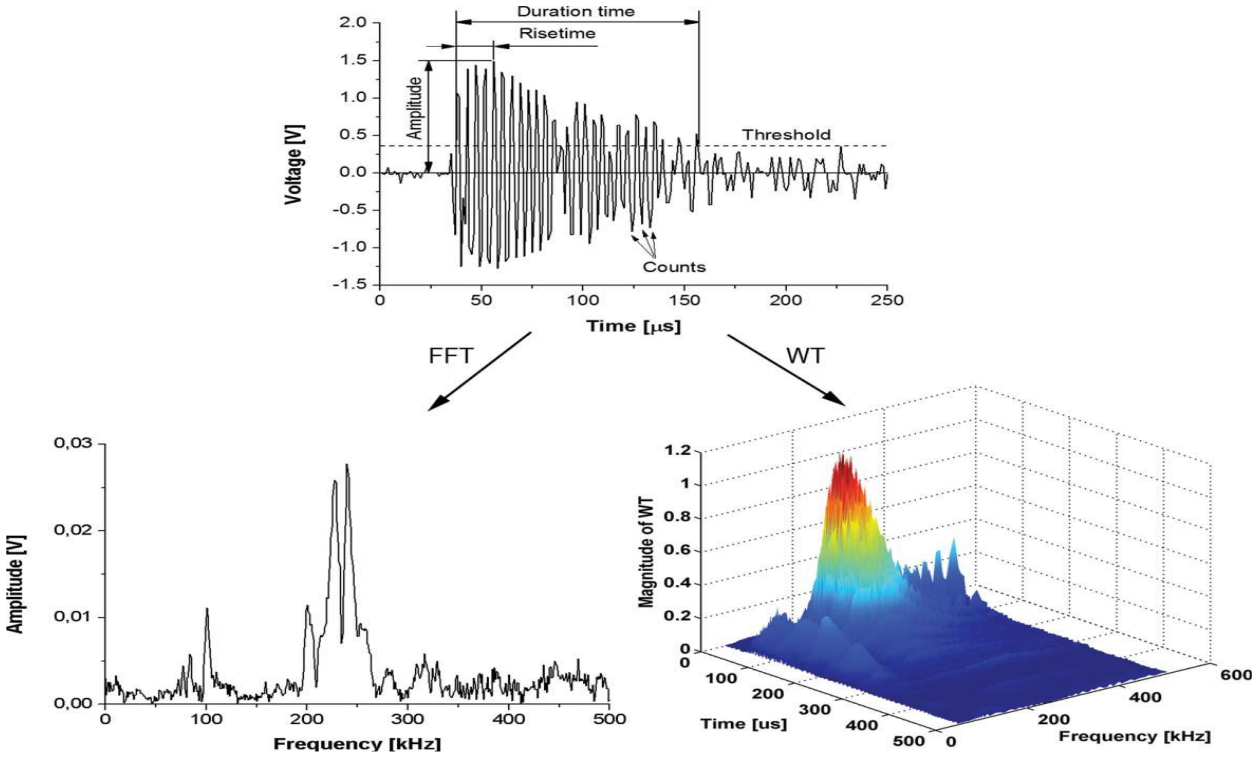

Figure 4. 9. The Characteristics of a Recorded Burst-type AE Event [41].

5. INVESTIGATIONS ON (FIBER GLASS / POLYMER) SPECIMEN

Fiber reinforced composite is a rapidly growing class of materials because of the importance of having low weight with high strength material. Mainly, polymer matrix reinforced with fibers, such as glass, carbon, or aramid is extensively used in almost all engineering sector applications. As reinforcement, the fiber is the most commonly used with ceramics, metals, and polymers to have materials with the advantages of high strength, stiffness, toughness, wear and corrosion resistance, and reduced cost. Namely, GFRP Material is used as specimen with definite dimensions to do our tests. Thus, the material was theoretically investigated to have an overview of it. The investigations done are studying the influence of the fiber size on the unit cell design of such material and doing a micromechanical analysis on a lamina of such material.

5.1. *Optimization of the Fiber Size for a Fiber Glass – Epoxy Composite*

5.1.1. Introduction

Over decades, many works of literature have been done to investigate the influence of the size of different types of fibers on the overall characteristics of the composite materials. S. T. Pinho [42] studied the effect of fiber size on the strength and toughness of fiber reinforced composite. F. Ramsteiner [43] investigated the influence of fiber diameter on the tensile behaviour of short-glass-fiber reinforced polymers. Hamdullah Çuvalci [44] has researched the effect of glass fiber content on the mechanical properties of a composite material. These researchers and others have confirmed that the fiber diameter has significant effects on the mechanical characteristics of the composite materials.

Glass fiber reinforced plastic (GFRP), e.g., Glass fiber / Epoxy is a class of plastic matrix composites that is reinforced by glass to mechanically enhance strength and stiffness of plastics. The resin (matrix) supports the fiber and adds more protection because of its ability of providing bonding between the two materials. As a result, GFRP presents flexible option for structural design due to its accessibility of manufacturing, high durability and structural efficiency (strength to weight ratio), and low production cost [45, 46]. Thus, the GFRP use has significantly expanded to the structural parts of airplanes, automobiles, marine, civil construction industries, sport goods.

Although, when designing composite materials, it is normal to take the matrix characteristics into account, in such cases, the essential factors which make changes in the material features are fiber size (diameter, length), fiber orientation, fiber contents and others [47]. This work studies the relationship between the fiber diameter (optimum) and the longitudinal tensile strength when designing materials based on representative volume element (RVE) or a unit cell, using an optimisation algorithm.

Swarm intelligence optimisation algorithms are used to estimate the optimal size of the glass fiber of circular cross-section of a glass-epoxy composite. Finding the best fiber size in a composite material has significant benefits on cost reduction. A comparative study was done to select optimal fiber diameter that can satisfy the optimal longitudinal tensile strength. Particle Swarm Optimisation algorithm (PSO) and artificial bee colony algorithm ABC are proposed for this comparative study.

5.1.2. Multi Scale Approach

Traditionally, simulation models were developed for one specific scale of magnitude (Macroscopic, Microscopic or Nano). In practice, it would be impossible to compute the vibration simulation for GFRP parts in the micro scale, because of the very fine calculation model and the resulting huge number of elements. The general idea of the multi-scale approach is to de-fine a context between models of different scales by reasonably linking results of adjacent scales. The multi-scale approach is widely used in science [48].

In this case the multi-scale method is used to derive the material properties (Young´s modulus and density) in the macro-structure based on the detailed information in its micro-structure. The micro-structure corresponds to the scale in which heterogeneities can be modelled for several small and representative local sections of a part, while the macro structure of the part is modelled homogeneously with Young´s modulus and density values differing among defined sections.

In the macro scale model, it is assumed that the properties of each material point (node of the macro model) can be described by mapping information from a representative volume element (RVE). This approach was firstly suggested by Drugan and Willis [49]. This RVE contains the information of underlying the inhomogeneous microstructure. Original material properties like Young`s Modulus and density are used for a classical solid mechanic analysis of the inhomogeneous RVE. In a homogenization step substitute Young`s Modulus and density are determined for the RVE based on the equivalence of stress and strain. These new substitute properties are called Boundary Conditions (BC) for macro nodes and are mapped to the relevant nodes of the macro scale model (Figure 5.1).

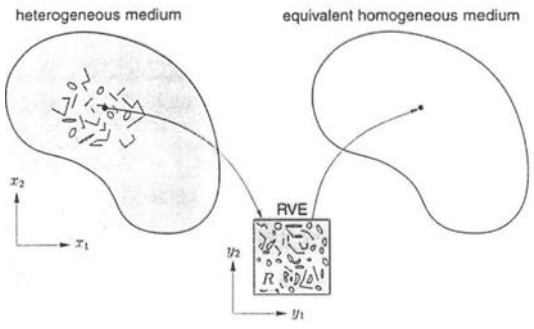

Figure 5. 1. Overview of Multi-scale Approach.

A Mean-Field Homogenization (MFH) is used in this step, which is based on the relation between volume averages and stress or strain fields in each phase of a RVE. In first-order homogenization substitute materials are computed with real constitutive

rules (constant volume, density and energy). A typical example of MFH is the Mori-Tanaka model [50] which is successfully applicable to two-phase composites with identical and aligned with ellipsoidal inclusions. The single inclusion problem (2D) was solved analytically by J.D. Eshelby [51]. 3D application has to be solved numerically (double inclusion problem). The model assumes that each inclusion of the RVE behaves as if it was alone in an infinite body made of the real matrix material. The BCs in the double inclusion problem correspond to the volume average of the strain field in the matrix phase of the real RVE.
Depending on the possible periodic distribution of the fiber in the composite materials, the RVE or unit cell might be of square or hexagonal packing array as shown in (Figure 5.2).

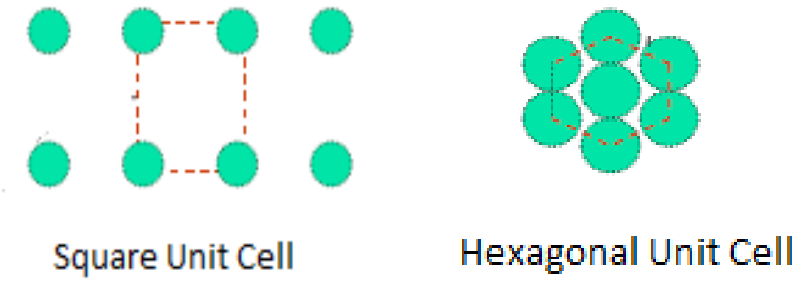

Figure 5. 2. Schematic Representation of Unit Cells.

In the theory of composite materials, the unit cell is modelled based on assumption such as the homogeneity of the composite material [11]. Taking into consideration the square unit cell with four fiber arrangement (Figure 3), the longitudinal tensile strength can be calculated using the equation:

$$F_{1t} = F_{ft}\left(v_f + \frac{E_m}{E_f}\right)(1 - v_f) \tag{5.1}$$

where :
F_{1t}*: Longitudinal Tensile Strength*
F_{ft}*: Fiber Tensile Strength*
v_f*: Fiber Volume Fraction*
E_m*: Matrix Young's Modulus*
E_f*: Fiber Young's Modulus*

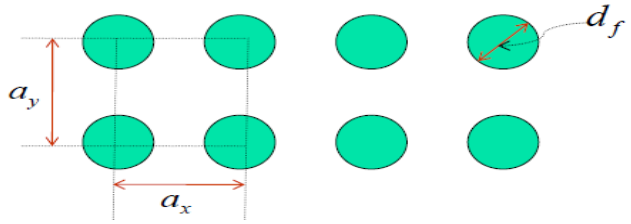

Figure 5. 3. Square Unit Cell with Four-Fiber Arrangement.

Since the volume fraction of the fiber is:

$$vf = \frac{\text{volume of the fiber}}{\text{total volume}} = \frac{\frac{\pi}{4}(df)^2}{ax.ay} \tag{5.2}$$

A direct relationship exists between the fiber and the longitudinal tensile strength.

5.1.3. Classification and Characteristics of the Glass Fiber

The two phases of the material were chosen to be glass as fiber and epoxy as a matrix. The classifications of the most used glass fibers with their physical properties are shown below.

Table 5. 1. Glass Fiber Main Classes and the Physical Properties.

Class of GF	**Physical Properties**
E-Glass	Higher strength and electrical resistivity
S-Glass	Highest tensile strength
R-Glass	Higher strength and acid corrosion resistance
C-Glass	Higher Corrosion resistance
D-Glass	Low dielectric constant

Based on equation (5.1), mechanical characteristics of the fiber and matrix are needed regardless of the fiber diameter which determines the volume of the fiber consequently by the fiber volume fraction (V_f). These characteristics are Fiber Young's Modulus (E_f), Matrix Young's Modulus (E_m), and Fiber Tensile Strength (F_{ft}). Table 2 shows the required characteristics of the glass fiber.

Table 5. 2. Glass Fiber Characteristics.

Glass Fiber	***Ef, GPa***	***Fft, GPa***
E-Glass	72.35	3.45
S-Glass	85	4.8
R-Glass	86	4.4
C-Glass	69	3.31
D-Glass	55	2.5

5.1.4. Classification and Characteristics of Epoxy

The contribution of epoxy resins in the composite material is by producing strength, durability, and chemical resistance. Their performance at elevated temperature with hot and wet service is high. Because of the outstanding adhesive ability that the epoxies have, they are able to bond very well with different types of fiber producing composite material with attractive properties. From this point, epoxies are taking a major part in the polymer matrix use for composite materials. Epoxy resin is widely used as a structural matrix in high-performance polymer composites for aeronautical and

astronautical applications. According to many literatures, epoxy resins are classified to many types. The table below presents some types of epoxies as a matrix with their modulus of elasticity that required for equation (5.1).

Table 5. 3. Epoxy Characteristics.

Epoxy	***Em, GPa***
8551-7	4.098
8552	4.667
9310/9360 @23c	3.12
9310/9360 @149c	1.4
9420/9470 (A) @23c	2.66
9420/9470 (B) @23c	2.83
HPT1072/1062-M @23C	3.383

5.1.5. Optimization Algorithm

Particle swarm optimisation PSO is a powerful and efficient optimisation algorithm which is widely used for a wide range of applications. PSO mimics the swarm behaviour of fish and birds, we can call the members of the swarm and the swarm itself as particles and population respectively, and every agent is a candidate solution to the optimisation problem. The position and velocity of a specific particle is denoted by:

$x_k(t) \in x$

$v_k(t) \in x$

where *k* is the index of the agent in the swarm and *x* is the search area while (*t*) is the iteration number of the algorithm. The standard PSO is as follows

$$x_{kj}(t+1) = x_{kj}(t) + v_{kj}(t+1) \tag{5.3}$$

$$v_{kj}(t+1) = w * v_{kj}(t) + r_1 C_1 (p_{kj}(t) - x_{kj}(t)) + r_2 C_2 (G_j(t) - x_{kj}(t)) \tag{5.4}$$

- $v_{kj}(t+1)$: denote the velocity of particle k in time step (t+1) and the jth component for this velocity
- r_1, r_2 : a random number in the range 0 to 1
- C_1, C_2 : acceleration coefficient
- w: inertia coefficient
- $w * v_{kj}(t)$: inertia term
- $r_1 C_1 (p_{kj}(t) - x_{kj}(t))$: cognitive component
- $r_2 C_2 (G_j(t) - x_{kj}(t))$: social component
- Equations (5.1) and (5.2) are the main rules that PSO employ for the search process.

5.1.6. *Optimization Problem*

Strength problem is a maximisation optimisation problem which depends on six main parameters, and the whole issue can be described as follow:

Consider $\vec{x} = [x_1 \quad x_2 \quad x_3 \quad x_4 \quad x_5 \quad x_6] = [d \quad a_x \quad a_y \quad E_m \quad F_{ft} \quad E_f]$

Maximise

$$f(\vec{x}) = f_{1t} = F_{ft}\left(v_f + \frac{E_m}{E_f}\right)(1 - v_f) \tag{5.5}$$

Subject to

- $v_f \leq 0.6$
- $F_{1t} \leq 2.5\ GPa$
- $5 * 10^{-6} \leq d \leq 40 * 10^{-6}$
- $50 * 10^{-6} \leq a_x \leq 100 * 10^{-6}$
- $50 * 10^{-6} \leq a_y \leq 100 * 10^{-6}$
- $2 * 10^9 \leq E_m \leq 5 * 10^9$
- $2 * 10^9 \leq F_{ft} \leq 5 * 10^9$
- $40 * 10^9 \leq E_f \leq 80 * 10^9$

The above-mentioned constraints were chosen based on characteristics in Table 5.2 and Table 5.3 considering the minimum and maximum values in these tables. Figure 5.4 shows the performance of PSO on this constrained optimisation problem where it is required to find the best possible set of variables that can meet the requirement of the constraints. It is worth to mention that for the set of variables in Table 5.4, the corresponding maximum F_{ft} is 2.8241e+09 while v_f is 0.5027.

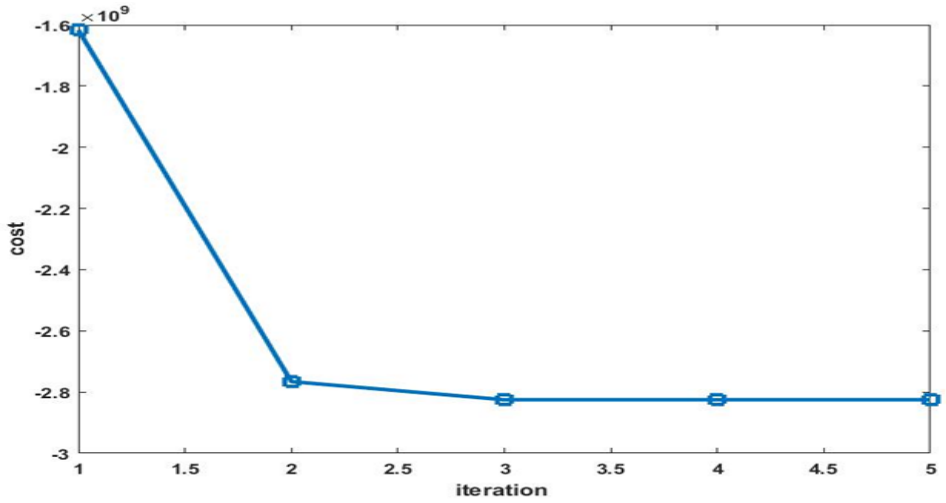

Figure 5. 4. The Convergence of the PSO on Maximum Strength Equation.

Table 5. 4. Best Possible Results for the Constrained Problem.

Parameter	***d mm***	***ax mm***	***ay mm***	***Em. GPa***	***F_{ft}. GPa***	***E_f. GPa***
Value	4.0e-05	5.0e-05	5.0e-05	5	5	40

5.1.7. Conclusion

Design of composite material based on micromechanical analysis was adapted. Micromechanical analysis evaluates the characteristics of heterogeneous composite layer by representing it as homogeneous – anisotropic material. The analysis estimates the overall properties of the composite depending on other known (by tests) characteristics of the material. So, it determines the strength and stiffness of the composite with in the fiber, matrix, and the interface. Micromechanical analysis is done under assumptions such as that the fibers are distributed periodically, the fibers are infinitely long, and each layer of the materials has homogeneity of orthotropic properties. Square RVE (unit cell) was adapted in this work.
Optimum design of Glass fiber-Epoxy composite material has been conducted through this study. Particle swarm optimisation was used to find the best design parameters including spatial elements of the unit cell as well as a given set of strength values for both Glass-fiber and Epoxy. For this problem, under given constraints, PSO was efficient enough to find the best possible design parameters within only five iterations.
The longitudinal tensile strength was optimally calculated considering the constraints of the problem such as the fiber volume fraction which was found as 0.5027 as optimum. From that, optimum diameter of fiber and the dimensions of the square unit cell were also found based on equation (5.2).

5.2. *Micromechanical Analysis of Glass Fiber/Epoxy Lamina*

5.2.1. Introduction

When designing a composite material, the properties can be controlled by many parameters such as fiber or matrix content (volume fraction), fiber size and spacing, layer sequence and fiber orientation. The achievement of required properties is based on selecting among the above parameters. For example, the strength in the fiber direction of unidirectional composite materials is larger than this in other direction and there is a linear increment between the fiber volume fraction and the longitudinal Young modulus [52]. Researchers have done a lot of work on determining the properties of composite materials by developing many analytical and numerical methods and models. Rule of mixture or inverse rule of mixture and Halphin-Tsai are approaches of the analytical methods. Numerical approaches include the unit cell methods and periodic microstructure methods [52–57].
Current work deals with the evaluation of the engineering constants such as longitudinal young modulus E_1, transverse young modulus E_2, in plane shear modulus G_{12}, and Poisson ratio V_{12} of unidirectional fiber reinforced composite. These properties are calculated by theory of elasticity based on a representative volume element (RVE) or a unit cell. The methods used are the rule of mixture (ROM),

Halphin-Tsai, cylindrical assemblage model (CAM), and periodic microstructure model (PMM). A square unit cell was adopted to carry out the micromechanics calculation in this work.
Current work investigates the mechanical behaviour of a unidirectional fiber reinforced polymer composite lamina consisting of fibers embedded in epoxy resin as a matrix. Micromechanical analysis is done on a square-patterned unit cell of the above composite to predict the longitudinal modulus (E_1), Transverse modulus (E_2), In-plane shear modulus (G_{12}) and Major Poisson's ratio (V_{12}). These engineering constants are evaluated to three types of fiber (E-Glass, R-Glass, and S- Glass) with various fiber volume fraction based on theory of elasticity approach. Computer Aided Design Environment for Composites (CADEC) software is used to do the numerical analysis. This theoretical investigation helps to realize the bearing ability of unidirectional fiber reinforced composite subjected to longitudinal load by analyzing the engineering design constants.

5.2.2. Micromechanical Analysis

The purpose of micromechanics is to study composite materials, considering the constituent materials interaction in detail. It lets the analyzer to compute the characteristics of a heterogeneous composite layer or a lamina by representing it as a homogenous-anisotropic material [58]. Furthermore, it determines the stiffness and strength of a composite material by studying the stresses and strains at a micro-structural level for the fiber, matrix, and the interface of the fiber and matrix. The results of micromechanics help to understand the load sharing between the constituents, the fiber arrangement of the composite and its influence on the material, as well as helping the designer to predict the average properties of the lamina and design the material by predicting the constituent content (volume fraction), their distribution and orientation [59]. To carry out the micromechanics analysis, there are assumptions that must be taken into account such as that the fibers are distributed in a periodic fashion within the matrix, fibers are infinitely long, each layer has orthotropic properties, and the bonds between the fibers and matrix are perfect.

5.2.3. Methodology

The focus of current work is to evaluate the engineering properties of a fiber reinforced composite material of a unidirectional fiber based on square array of RVE. The analysis is done using analytical methods such as rule of mixture, Halphin-Tsai, cylindrical assemblage model CAM, and periodic microstructure model PMM. These methods were used individually to calculate modulus in the direction of the fibers E1, modulus in the transverse-to-fiber direction E_2, In-plane shear modulus G_{12}, and In-plane Poisson's ratio V_{12}. All calculations are done based on the assumption that the material is anisotropic and homogenous and all formulas are applied to a unit cell [59].

Rule of Mixture

For a unit cell, the longitudinal modulus:

$$E_1 = E_f V_f + E_m V_m \qquad (5.6)$$

Poisson's ratio:

$$V_{12} = V_f V_f + V_m V_m \quad (5.7)$$

where:
E_f: Fiber elastic modulus
V_f: Fiber volume fraction
E_m: Matrix elastic modulus
Vm: Matrix volume fraction
V_f : Fiber Poisson's ratio
V_m : Matrix Poisson's ratio
V_{12}: Poisson's ratio for plane 1-2

Inverse Rule of Mixture

The modulus that is perpendicular to fiber direction (Transverse Modulus) E_2:

$$\frac{1}{E_2} = \frac{V_m}{E_m} + \frac{V_f}{E_f} \quad (5.8)$$

Halpin-Tsai Equation

The results of this equation are more accurate and beneficial for analytical evaluation and design purposes

$$E_2 = E_m \left[\frac{1+\zeta \eta V_f}{1-\eta E_f}\right] \quad (5.9)$$

where:

$$\eta = \frac{\frac{E_f}{E_m} - 1}{\frac{E_f}{E_m} + \zeta} \quad (5.10)$$

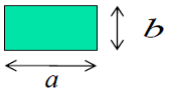

$\zeta = 2$ for circular and square fiber, $\zeta = 2\frac{a}{b}$ for rectangular fiber

Cylindrical Assemblage Model (CAM) Formula

Shear Modulus in the 1-2 Planes G_{12}:

$$G_{12} = G_m \left[1 + \frac{V_f \left(1 - \frac{G_m}{G_f}\right)}{\frac{G_m}{G_f} + S_3 \left(1 - \frac{G_m}{G_f}\right)}\right] \quad (5.11)$$

where: G_m: Matrix Shear Modulus
G_f: Fiber shear modulus

Periodic Micro-Structure Model (PMM) Formula

$$G_{12} = G_m \left[1 + \frac{V_f \left(1 - \frac{G_m}{G_f}\right)}{\frac{G_m}{G_f} + S_3 \left(1 - \frac{G_m}{G_f}\right)} \right] \qquad (5.12)$$

where: $S_3 = 0.49 - 0.47V_f - 0.027\ V_f^{\,2}$.[59]

5.2.4. Materials

The study is carried out on three types of materials which are E-galss/Epoxy, S-glass/Epoxy, and R-glass/Epoxy with different fiber volume fraction Vf, and the results are compared and analyzed.

Glass fiber in general is formed from bulk glass. Glass is an amorphous substance manufactured from a blend of sand, limestone, and other oxidic compounds. Thus, the main chemical constituent of glass fibers (45–75%) is silica (SiO2).

There are various types of glass fibers have been found by controlling the chemical composition and the manufacturing processes [59]. All types can have the typical glass properties such as hardness, corrosion resistance, light weight, and low cost, leading to make glass fibers one of the most used fiber in industrial composite materials. The glass fiber types are E, D, C, S, and R glass which they all have similar stiffness but different strength and different resistance atmosphere degradation resistance. The types used in this study are E-glass (E for electric) which used with applications that need high strength and high chemical resistance. S-Glass (S for strength), has high strength but it is very costly comparing with other types. R- Glass is the European version of American high-performance S-Glass. It is distinguished by the high strength and modulus, high temperature resistance, and good fatigue stability [60].

Table 5. 5. Chemical Compositions of Glass Fibers In wt%.

Type	(SiO_2)	(Al_2O_3)	Tio_2	B_2o_3	CaO	MgO	Na_2O	K_2o
E-glass	55.0	14.0	0.2	7.0	22.0	1.0	0.5	0.3
S-glass	65.0	25.0	n.d	n.d	n.d	10.0	n.d	n.d
R-glass	60	24	n.d	n.d	9.0	6.0	5.0	0.1

Table 5. 6. The Properties of the Used Constituents of the Composite Materials.

Material	Modulus (GPa)	Poisson's Ratio
E-Glass	72	0.22
S-Glass	85	0.22
R-Glass	86	0.25
Epoxy	4.667	0.35

5.2.5. *Results and Discussion*

Current analysis tries to distinguish among three types of laminas consisting of glass fibers embedded in epoxy matrix, by evaluating the engineering constants. The three types of glass fibers are E-glass, S-glass, and R-glass. Different Micromechanics formulas based on different approached are used to predicts some of the constants and then study them by comparing between the results.
The longitudinal modulus is evaluated for all types of materials by the ROM methods and a comparison among the results is made as shown in the Figure 5.5.

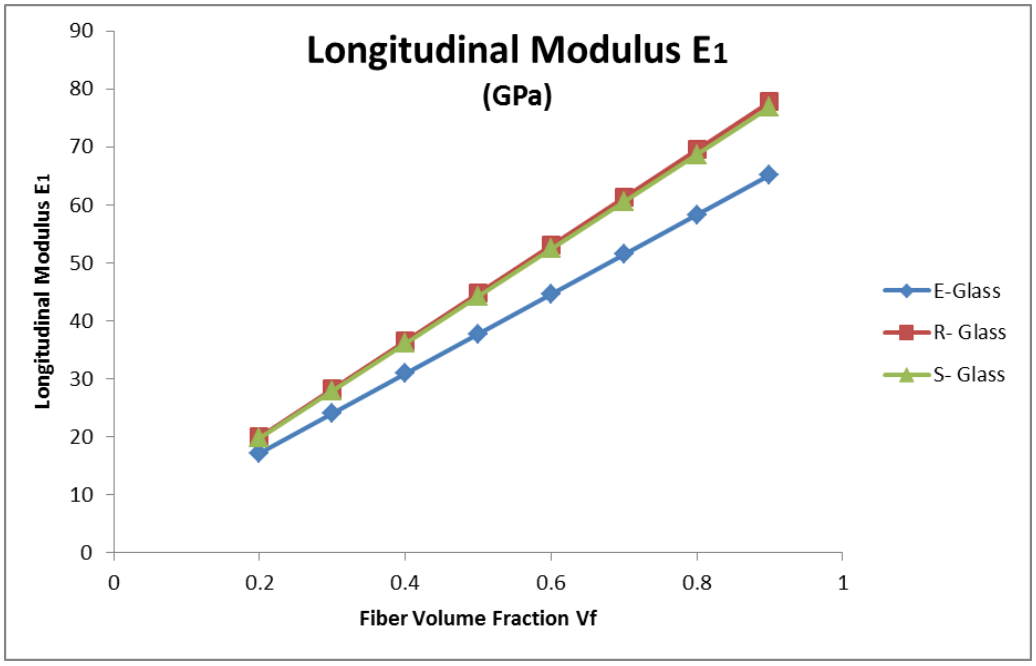

Figure 5. 5. Variation of E_1 with Fiber Volume Fraction for all Fibers.

- For all suggested volume fractions v_f, the longitudinal young's modulus E_1 of the E-glass / Epoxy is lower than those of R-glass / Epoxy and S-glass / Epoxy which they seemed to have very close young's modulus all over the variation of v_f. (see Fig.5.6).
- The longitudinal young's modulus E_1 increases linearly with increase in fiber volume fraction for all the three types of composites materials proving the fact that the strength of the unidirectional fiber composite is as high as the fiber volume fraction high since the fiber is stiffer and stronger.

As shown in the Figures 5.6-5.14, that for each material the transverse modulus E_2 is calculated in two ways, rule of mixture ROM and Halphin-Tsai.
The in-plane shear modulus G_{12} is evaluated by the cylindrical assemblage model CAM and the periodic microstructure model PMM.
The in-plane Poisson's ratio for each type of materials is calculated based on the ROM and PMM.
Comparison is made between each two different results of each constant. Furthermore, variation of longitudinal young modulus with the volume fraction for all types of composite materials is done. From above graphs, some findings can be stated

(E-Glass / Epoxy lamina)

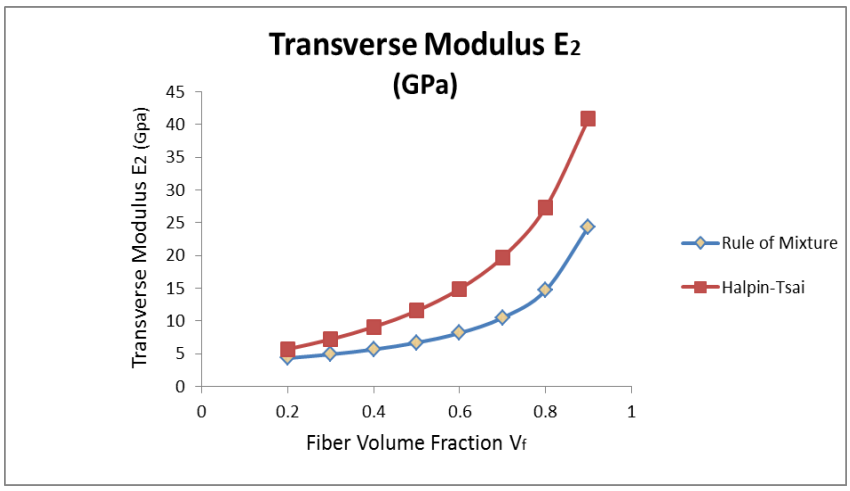

Figure 5. 6.Variation of E2 with Fiber Volume Fraction.

- The transverse young's modulus E_2 increases linearly with increase in fiber volume fraction for all the three types of composites materials up to 80 % of volume fraction and rapid increase happens after that.
- For all three types of materials, the magnitude of E_2 computed by ROM is much lower than this computed by Halphin-Tsai methods for all fiber volume fractions, pulling to the mind the fact that the ROM equation under-estimates the actual value for E_2 while the Halphin-Tsai methods gives more accurate results of it (see Figs.5.6, 5.9, 5.12).

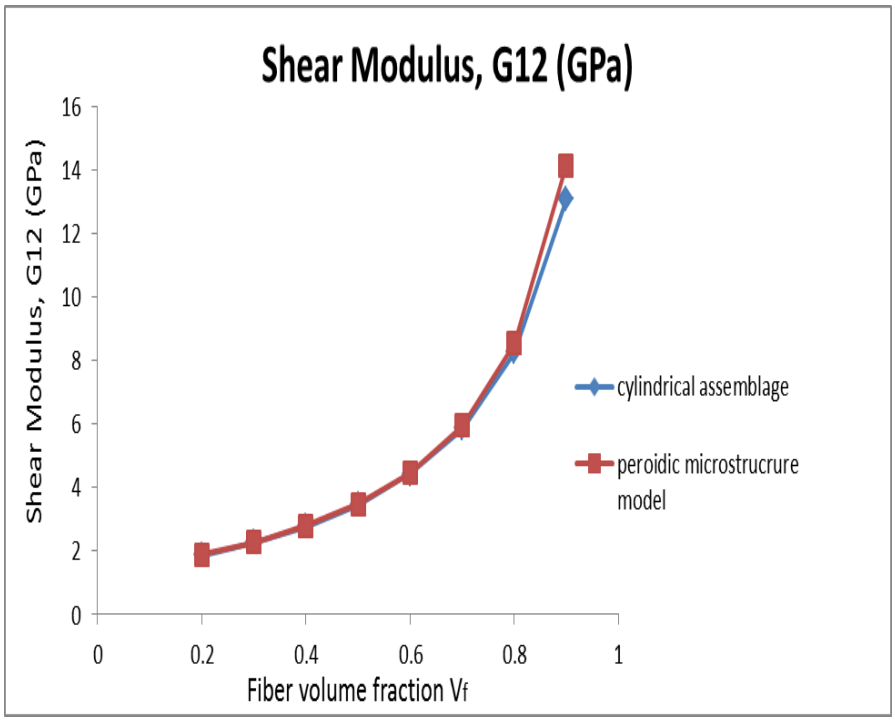

Figure 5. 7. Variation of G_{12} with Fiber Volume Fraction.

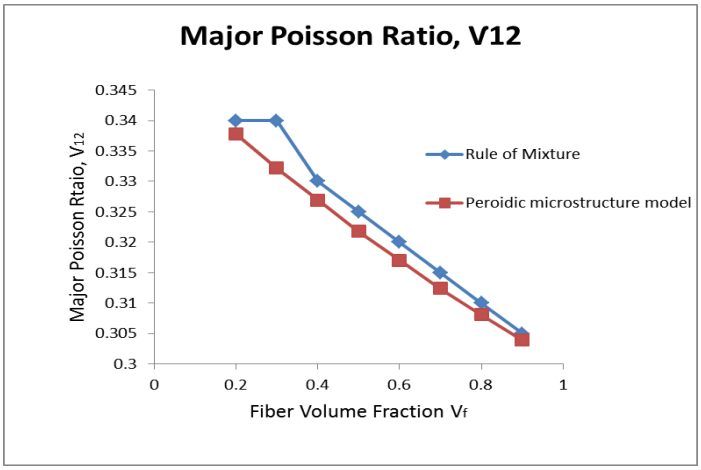

Figure 5. 8. Variation of V_{12} with Fiber Volume Fraction.

(R- Glass / Epoxy lamina)

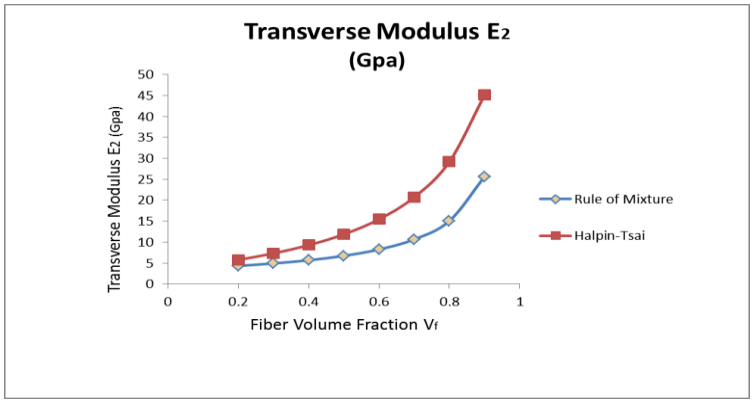

Figure 5. 9. Variation of E_2 with Fiber Volume Fraction.

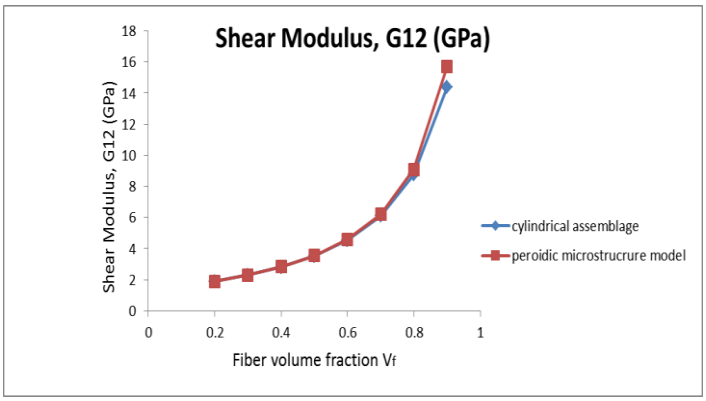

Figure 5. 10. Variation of G_{12} with Fiber Volume Fraction.

- In plane shear modulus G12 increases linearly with increase in fiber volume fraction for all the three types of composites materials, but, after 80% of the Vf,

there is noticeable difference of G12 computed by CAM and PMM methods (see Figs.5.7, 5.10, 5.14).

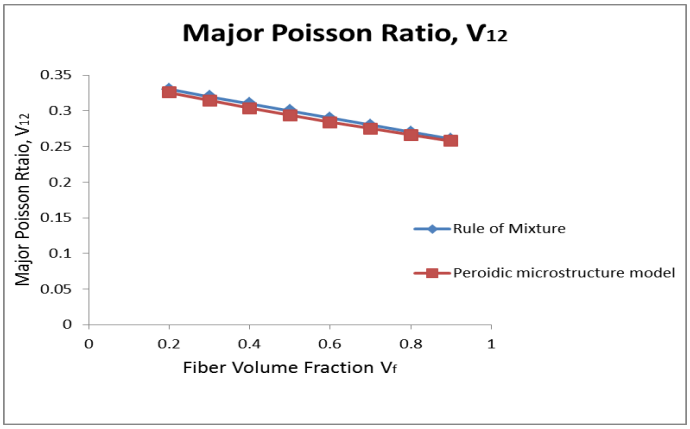

Figure 5. 11. Variation of V_{12} with Fiber Volume Fraction.

(S- Glass / Epoxy lamina)

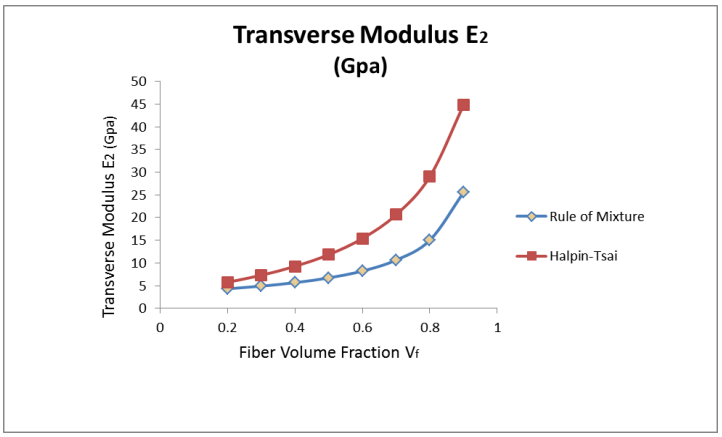

Figure 5. 12. Variation of E_2 with Fiber Volume Fraction.

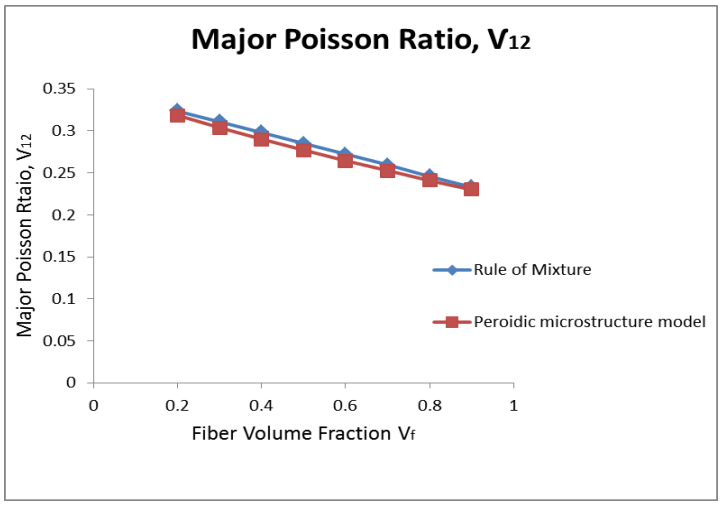

Figure 5. 13. Variation of V12 with Fiber Volume Fraction.

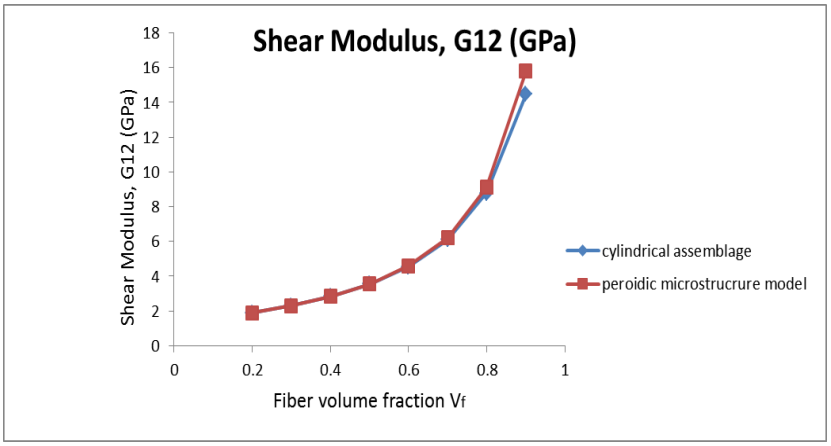

Figure 5. 14. Variation of G_{12} with Fiber Volume Fraction.

- For all composites, Poisson's ratio ν_{12} is decreasing with increasing the fiber volume fraction. However, for E-Glass/Epoxy, the magnitude of ν_{12} computed by ROM tries to stay at same level at the beginning of the curve, but rapid decrease happens after that making noticeable difference with the magnitude of this computed by PMM (see Figs.5.8, 5.11, 5.13).

Generally, it can be seen that the longitudinal modulus E1 is increasing with the increase of fiber volume fraction. Also, there is a linear increment of the transverse modulus E2 with the increment of fiber volume fraction. In addition, in plane Shear modulus G12 increases linearly with increase in fiber volume fraction for all the three types of glass fibers. However, for all composites, Poisson's ratio ν_{12} is decreasing with increasing the fiber volume fraction.

5.2.6. Conclusion

This work is carried out to evaluate several elastic constants for three types of unidirectional fiber reinforced composite materials (E-glass/Epoxy, S-Glass/Epoxy, R-Glass/Epoxy), using some approaches of composite materials micromechanics. Focus has been given to distinguish among the three types of the glass fibers. Square unit cell is used with all necessary assumptions and CADEC software is used to compute the engineering constants.

Elastic moduli E1 results are used to make comparison between the glass fiber types and are calculated using the ROM equation. The results of E2 are found using the ROM methods and Halphin-Tsai methods and are analyzed and compared between the three types. Moreover, G12 is evaluated using the two methods CAM and PMM with highlighting the results of each method. Poisson's ratio ν_{12} is also calculated with ROM and PMM for all three types of composite materials. Current theoretical investigation findings assist the designers and analyzers to expand their engineering knowledge about unidirectional fiber reinforced composite and its design process parameters. Future work will include a finite element results and comparison will be done. A macro-mechanics analysis of a laminate will also be of a future interest study.

6. EXPERIMENTAL MODAL ANALYSIS FOR INVISTIGATING THE NVH CHARACTERISTICS OF COMPOSITE VEHICLE COMPONENTS THROUGH VISIBLE AND NOT VISIBLE DAMAGES

6.1. *Introduction*

Composite materials, e.g., fiber reinforced polymers (FRP), are more and more utilized in the vehicle and machine industry. FRP components can show damages that are not visible after impact or crash. A component that is damaged (even not visibly) loses its load capacity, its original energy absorption capacity and its Noise, Vibration and Harshness (NVH) behaviour can change significantly.
This experiment presents the investigation of the Noise, Vibration and Harshness (NVH) behaviour of damaged and not damaged fiber reinforced polymer FRP test probes with simple geometry. For that purpose, artificial defect/failure generation procedure for the test probes will be developed and applied. Afterwards some NVH measures, e.g., natural frequencies, modal damping and mode shapes will be evaluated. The results will show on the one hand the sensitivity of the measurement method for damages and on the other hand the change of the NVH characteristics of the probes through damages.
In order to understand the change of the NVH behaviour of FRP vehicle components through certain damages (e.g., fiber or matrix cracks) for the first instance the investigation of simple test specimen is recommended. For that purpose, we organized overall 20 pieces of specimen, which makes the repetition of the planned investigations is possible, respectively do some statistics. The generation procedure of the damages on the specimen should be also considered. The high-speed impact of balls, bullets, etc. by means of drop tests, or gun seems to be simply realized.
One of the test methods, which can describe the NVH characteristics of a structure, is the modal analysis. The method delivers the modal frequencies, mode shapes and modal damping where the parameters can be more or less responsible for the NVH behaviour of a vehicle. If the excitation meets a modal frequency, and the mode shape at that modal frequency has good radiation efficiency or the path of vibration transfer from that part to another in the vehicle is sufficient, this method will be applied for the investigations. After getting the results of the modal test, they will be analyzed, and the change of the modal behaviour between undamaged and damaged specimen will be explained. At the end the eligibility, respectively the sensitivity of the modal analysis method for crack detection at FRP should be verified.
The general composition of FRP is fiber (carbon, glass, etc.) and resin (polymer). The common types of fibers are aramed, glass, carbon and basalt.
The resin can be of two categories:

- Thermoset Resins: it is common in structural uses. it cannot be reformed.
- Thermoplastic Resins: It has the property to be reformed.

Common Types of Thermoset Resin are polyester, vinyl ester, polyurethane, and epoxy.

6.2. *The Test Specimen*

For the further investigations we selected a glass reinforced plastic plate with the material type of MF GC 201 (melamine resin laminate) due to the simple accessibility, and similar types are often used by vehicles. The specimen had a simple rectangular shape with the dimensions of 500x200x3 mm (Figure 6.1).

Figure 6. 1. The Rectangular FRP Test Specimen.

6.3. *Possible Damages in Composites*

The mechanism of damages in composite materials is not easily predicted and understood due to the nature of the material. Defects and fracture generally may occur during the manufacturing process or service life of the structure or parts. The damage mechanisms in a fibrous composite are broadly categorized as:

A- Micro-level damage: This can be classified into fiber level damage and matrix level damage mechanisms. Regarding the both level, there are many damages occur such as (fiber breaking, fiber buckling, fiber bending, fiber splitting, and matrix cracking).
B- Macro-level damage: The macro-level mechanisms are laminate level mechanisms. It is seen that the adjacent layers are bonded together by a thin layer of resin between them. This interface layer transfers the displacement and force from one layer to another layer. When this interface layer weakens or damages completely, it causes the adjacent layers to separate. This mode of failure is called delamination.
C- Coupled Micro-Macro Level Failure Mechanisms: The through thickness transverse crack may propagate to neighbouring lamina causing it to break. (Ever 2010).

6.4. *Generation of Artificial Damage in the Composite Specimen*

In order to generate any type of damages (e.g., matrix cracks) in the material of the test specimen, several experiments were performed. For the first considerations we thought about a simple bearing ball drop test. Within our possibilities we could only reach roughly 8.5 m drop height in the building of our institute, which proved as not

sufficient to generate any damage. In this case the maximum kinetic energy of the falling ball with m = 20 g weight was approx. E_{kin} = 1.6 J. We also increased the ball weight to m = 40 g, resp. E_{kin} = 3.2 J, without success. We could not even find the place of the ball-specimen contact.
Thus, we utilized an air gun, type Diana 300R cal.177, which has the kinetic energy of E_{kin} = 7.5 J at the muzzle. The gun "fires" lead pellets with the weight of m = 0.53g with a calculated speed at the muzzle of 170 m/s. After firing with this air gun from 10 m distance we could find the contact place, with a small, flat buckle. The hit could be detected also on the back side of the plate. After the repetition of the shots from 7,5m, 5m, and 2,5 m we could only detect the small flat buckles without any cracks of the specimen.
At the next firing tests, we reduced the distance to the specimen to 1.5 m and we shot two times. At the first shot we could see only a small buckle (Figure 2 left: 1st impact), but by the 2nd shot the specimen has cracked, we could produce a crack with a length of 70 mm (Figure 6.2 left and right). So, we used that cracked specimen for the further investigations.

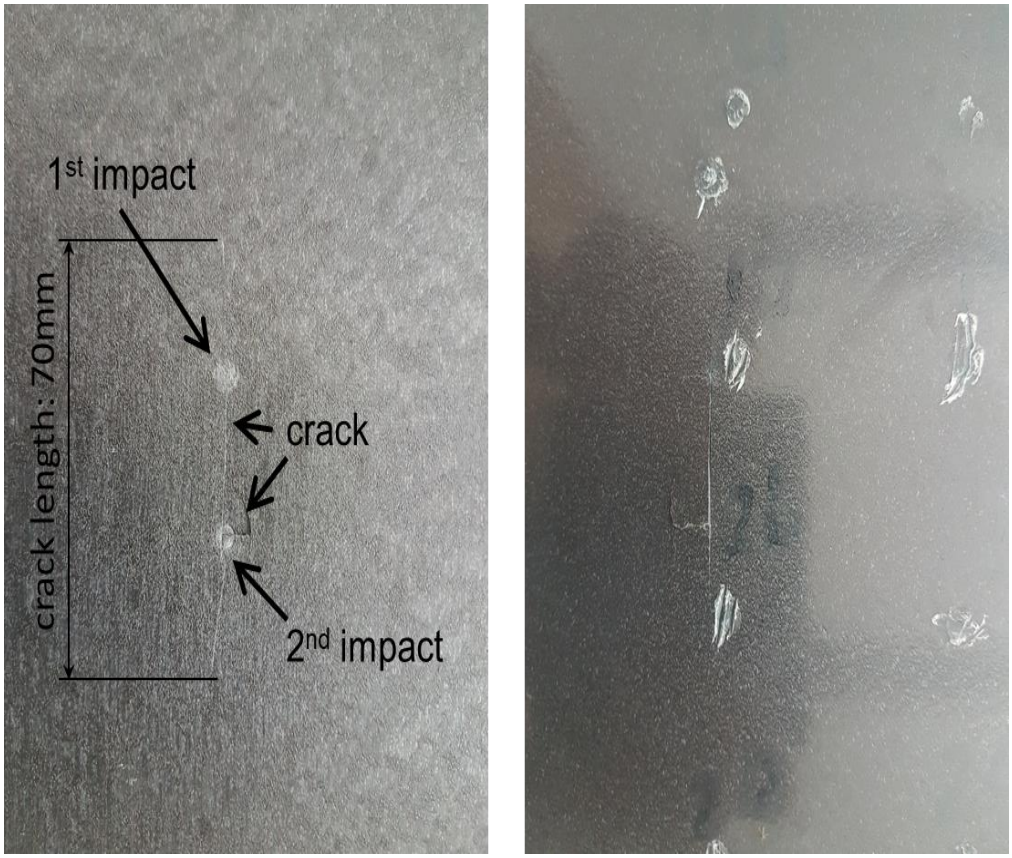

Figure 6. 2. Damage of the Specimen (left: side of the impact; right: back side)

6.5. *Methodology*

For many years, modal analysis has been used to investigate vibration characteristics of mechanical components, including aerospace components and rotational machinery. Lately, the field of modal testing has been extended towards testing of existing structures to comment on serviceability and loss in performance through eventual degradation of individual components. A gradual change in material performance,

promoted by the progression of the above-mentioned factors, will most likely result in changes in the variation characteristics. Herein, modal frequencies, mode shapes and damping properties of structural components. These can be extracted through modal testing, which has proven suitable for in-situ testing of structures, even on the large scale. In the following section, the methodology employed in modal testing will be outlined and discussed.

To excite a structure for modal measurements, two methods of excitation can be chosen, namely input-output (active excitation) and output only (operational excitation). Input-output methods of excitation involve a contact procedure in which an exciting function is introduced to initiate vibration of the structure. Typical forms of excitation entail impact hammers, drop weights, shakers or displacement-release.

The waveforms used in modal analysis can be of various natures, including harmonic and random input, as well as impulsive excitation. Output only excitation is present if the structure is in service and under some form of external excitation, e.g., traffic or wind loads.

In field testing, dynamic properties are extracted by placing several motion sensors (commonly accelerometers) at predetermined locations along the structure. To suit the need for full-motion recording, triaxial accelerometers are commonly given preference. The objective of placing sensors in multiple locations is to attain a sufficient amount of frequency response functions (FRF), such that individual modes can be identified from the modal test. Herein, the highest measurable mode depends largely on the optimal placement of accelerometers; i.e., the extraction of higher modes demands a higher number of accelerometers [61].

6.6. *Performing the Test*

Before performing the tests, we defined overall 30 measurement points on the plate, to be able to represent also the mode shapes, which tend to have more local displacement, than global. This number of points should be sufficient enough for that. The distance of the points was 50 mm along the long side, and 75 mm along the short side of the plate (visible on Figure 1.). Measurement point Nr. 30 was also the excitation point.

For the measurements we used test equipment B&K Pulse frontend, B&K Pulse Labshop, B&K 4397 uniaxial accelerometer, and Endevco 2202-10 impact hammer. We decided to perform the fixed hammer excitation method. The schematic representation of the measurement setup is described in Figure 3 [62]. We laid the plate on both ends on elastic foam supports and placed 1 accelerometer on the 1st measurement point. After that we hit on the excitation point, 10 times, the recorded FRFs were averaged. We repeated the measurement also for the remaining measurement points.

We checked during the test the quality of the FRFs, the coherences, the spectrum and time signal of the excitation (e.g., to avoid double hits). A typical FRF, coherence and auto power spectrum of excitation is shown in Figure 6.4. The quality of the measured seems to be ok, the excitation shows no significant drop of level over the frequency, the coherence, beside a few anti-resonances, is high, reaches the value of nearly 1. Before the test on the probe, which was cracked by the shots, we also performed the recording a few FRFs on 6 probes with the same material and dimension (incl. the probe which was cracked later). The goal was to see the scatter of the resonance frequencies on similar/same probes. The FRFs showed no significant differences between the resonance frequencies.

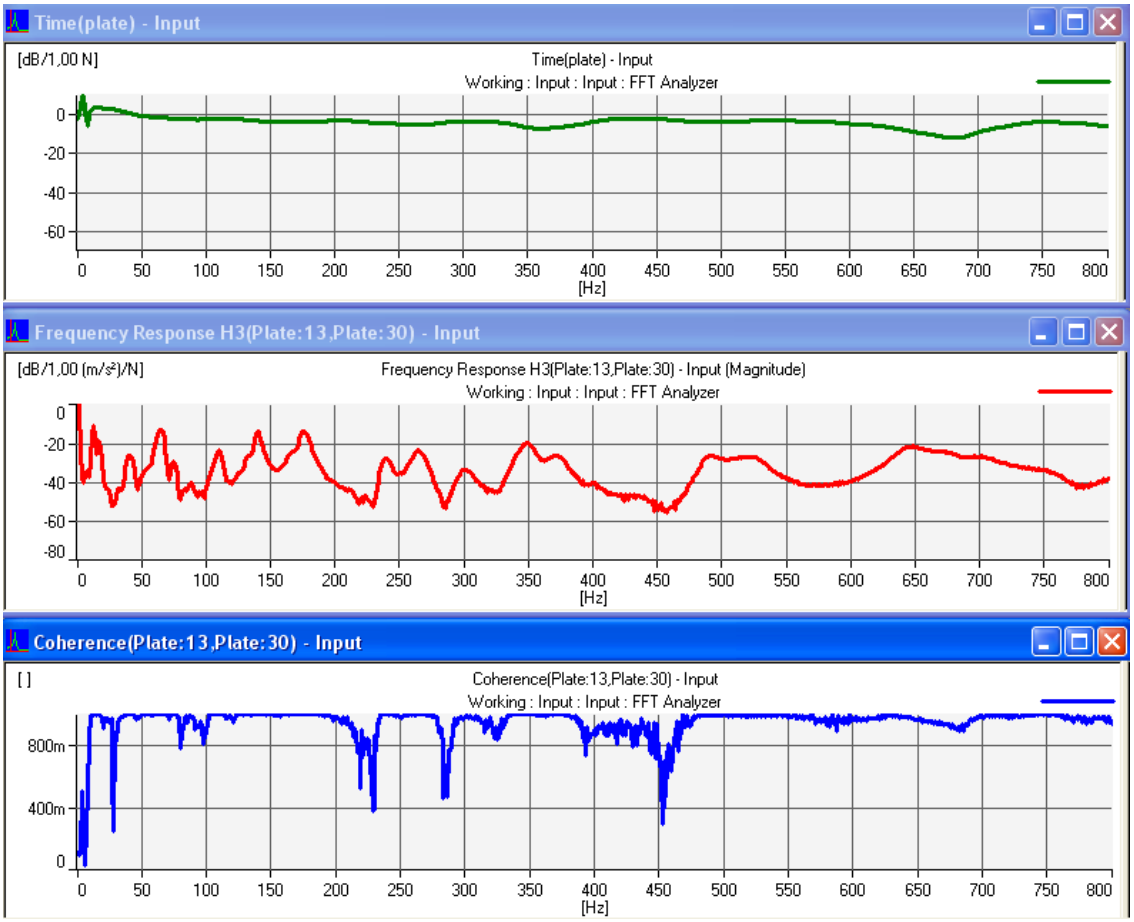

Figure 6. 3. Typical Excitation Spectrum, FRF and Coherence During the Measurements (upper: autopower of excitation; middle: FRF; lower: coherence).

6.7. *Results of the Test*

At first sight on the average of the transfer functions (Figure 6.5), no significant difference can be seen in the overall characteristics of the FRFs. From 550 Hz there is some difference, but this is rather due to the poor excitation level, and the high damping of the material. Beyond that frequency no more distinct resonances can be found in the FRFs.

If we look at the individual resonances (roughly 20 pieces up to 500 Hz) in the range from 110 to 190 Hz (Figure 6.6), differences in level of the peaks, and missing resp. new peaks can be found in the averaged FRF of the cracked plate compared to the uncracked one.

It can be stated that an existing crack in the material causes the appear and the disappear of certain resonances. Presumably the modes are not appearing/disappearing, they are always there, but due to the crack they will be simply better or worse excited, depending on the frequency, mode shape and damping.

By performing the complete modal analysis, the assumption before could be boosted. That means the resonance peaks changing (appearing or disappearing) significantly, where a large relative displacement between the measurement points in the surrounding of the crack of a mode shape can be observed. On our cracked specimen the crack is ranging approximately from the measurement point 14 to 20, and here also a large displacement can be observed.

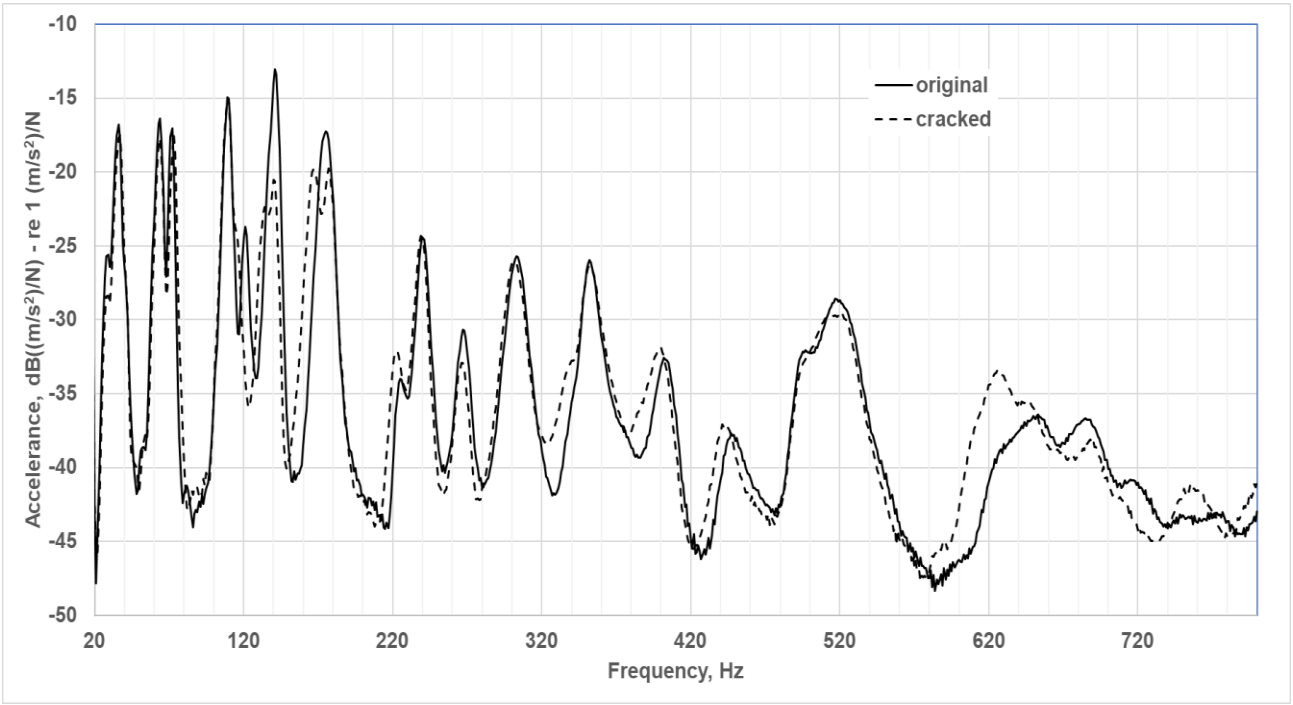

Figure 6. 4. The Average of the Measured FRFs for the Uncracked and Cracked Specimen (from 20 to 800 Hz).

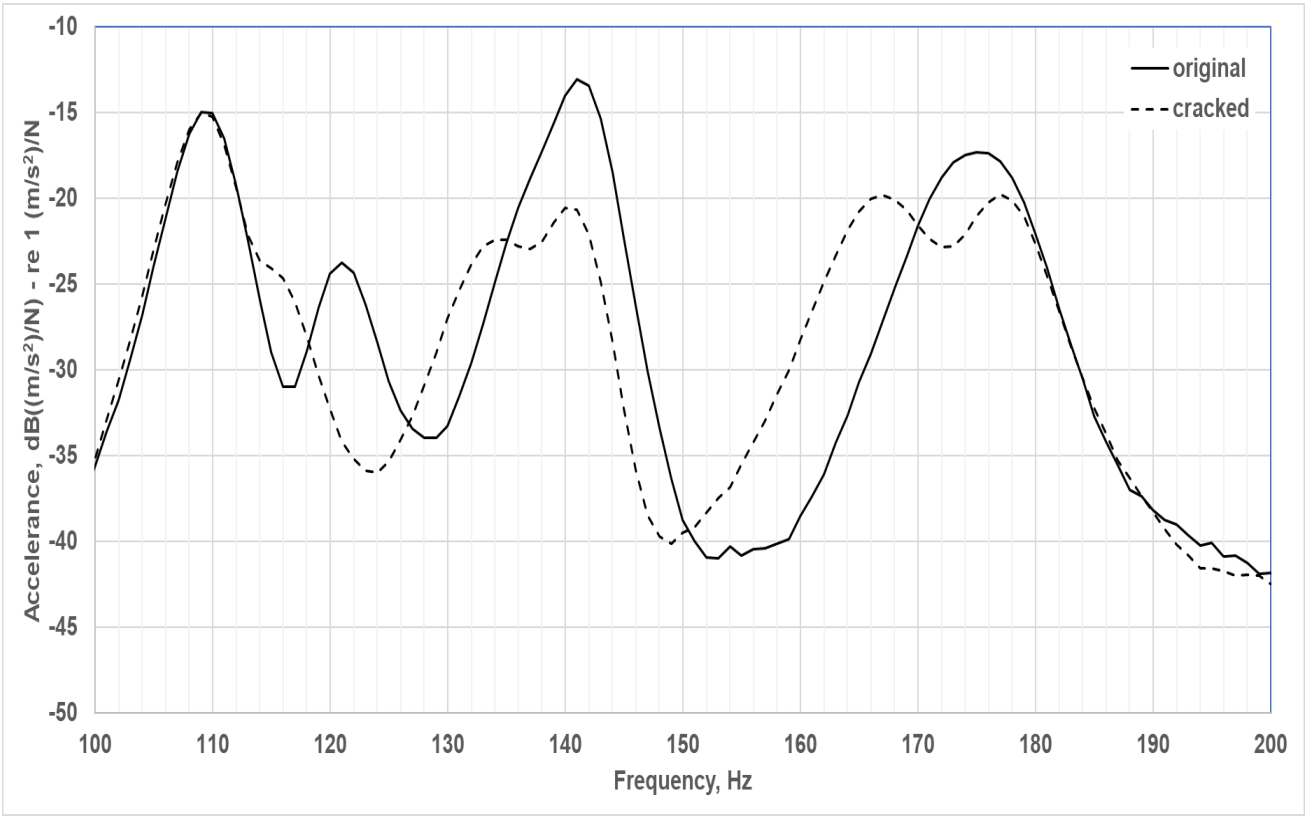

Figure 6. 5. The Average of the Measured FRFs for the Uncracked and Cracked Specimen (from 100 to 200 Hz).

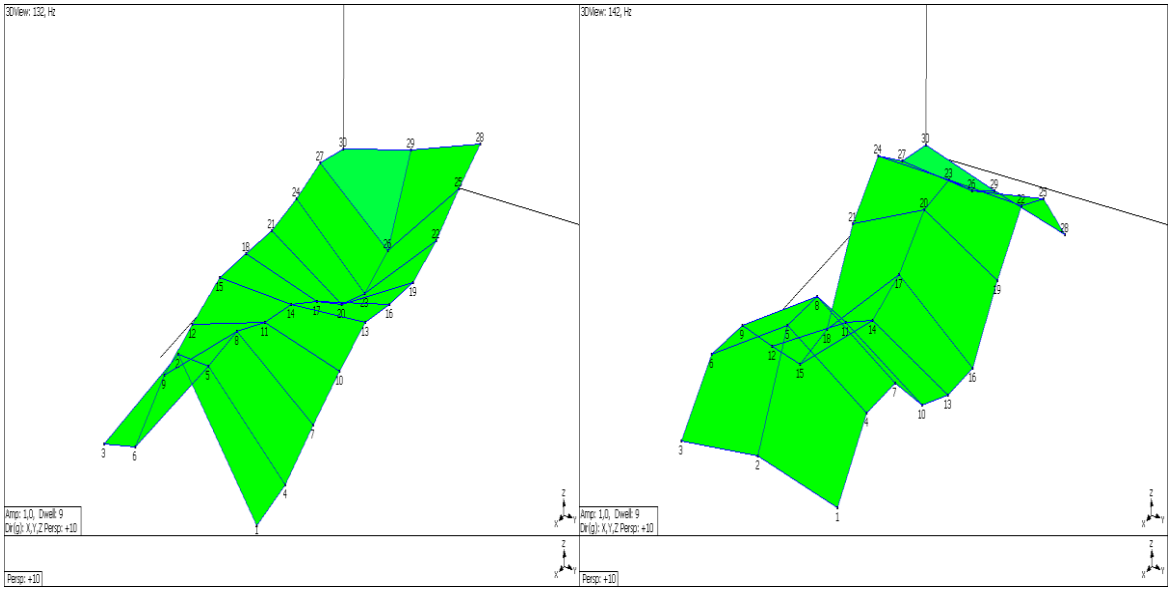

Figure 6. 6. Two Mode Shapes of the Cracked Plate by 132 Hz (left) and 142 Hz (right), Displacement in the Z direction.

6.8. *Conclusion*

The modal analysis can help in certain ideal conditions to detect a crack in FRP material. The method can only work in the low frequency range due to the poor excitation with impact hammers over 800 Hz. With an excitation with a light shaker this limit can be raised, but due to the gradually growing modal density the investigation of single resonances and modes will be difficult. In this case we know about the crack, so we were waiting some change in the modal behaviour of the specimen (the previous mentioned ideal condition). In real cases by a relatively complex shaped vehicle component other effects have to be considered, even a not optimal support of the component by the test can cause some change in the modal behaviour. The modal analysis still has to be more investigated for the purpose of crack detection in FRP, but also in general for other types of material. At the time of writing this work, only a single test is existing, so the test has to be repeated several times, in order to obtain the sensitivity of the method for external influences and for the crack generation.

7. DAMAGE DETECTION IN A FIBER REINFORCED POLYMER COMPONENT BY THE VIBRATION DECAY RATE AND THE DAMPING BEHAVIOUR

7.1. *Introduction*

Failures of composite materials due to poor anticipations of damages occur very frequently. Damages in composite materials may exist as visible or non-visible with different configurations and identities. Thus, investigation of damages existence in composite materials has to have a prior attention to avoid the failure of structures.
Damages may arise in the FRP components during operation putting the structure in a risk [7]. Due to the heterogynous microstructure of the materials and big difference of the constituent's properties, the mechanism of the damage is not smoothly predicted and understood. Also, the interface presence and the fiber orientations give anisotropy in overall properties of the materials [7, 8].
The diagnosed damages of composite materials are broadly classified under three main categories based on the structure of the material. These main categories are the micro-structure level, the macro-structure level, and the coupled micro-macro level mechanism failure. Under all three levels, the damages of composite materials could be [9]:

- Fiber Fracture
- Fiber Bending
- Fiber Buckling
- Matrix Cracking
- Delamination
- Fiber deboning
- Others.

In order to have an early prediction of existence of visible or non-visible damages in composite structure and avoid failure, many structural health monitoring (SHM) methods have been revealed. Among these methods are guided waves method, acoustic emission methods, wave field imaging, modal analysis, frequency response function method, and others [9, 10]. Thus, a lot of attention has been paid to the issue of damages detection in composite materials structures using acoustic emission and vibration-based methods [46, 63–69].
Vibration based damage detection methods are among the most widely used methods in the topic of SHM for composite structure [70, 71]. Many researchers have been studying the vibration characteristics in structural damage detections [72, 73] and particularly for composite structure [46, 63, 69, 74–78].
On the other hand, the damping properties of composite materials are superior to other metallic materials. Since, the assessment of damping properties of composites is not an easy process, they are not commonly considered in the design and analysis

processes[79]. Few researches and reviews were done regarding the topics of composite materials damping [80–82]. However, damping of composites is distinctly higher than that of other traditional engineering materials. Based on the designed composite part, the damping depends on the fiber properties, the matrix properties, the interface between them, the number of lamina and their sequence, and the attached viscoelastic layers if exist[83].
Considering that the damages of composite materials have an effect on the vibration decay rate, this chapter includes using the experimental measured decay rate to predict the damage presence on the specimen. The measured decay rate shows an estimation of the dynamic behaviour of the target part[84]. The focus of the current investigation is to do laboratory work for measuring the vibration decay rate of a FRP composite component.
In addition to that, Current chapter investigates the damping response offered by a damaged fiber reinforced polymer plate. The plate is put under three different conditions regarding the damage existence. The focus is to measure the loss factor in all cases and determine whether there is difference among them to prove damage presence in the composite part. The loss factor is experimentally measured by measuring the vibration decay time RT60. The resulted data of loss factor show a well distinguished difference that might lead to predict damages, and to do more expanded analysis of this issue.
The focus of this experimental investigation is to analyse damping response of a composite plate made of glass fiber reinforced polymer in order to predict damage existence.
The loss factor which is obtained through the measurement of the decay time RT60 is measured for the three cases of the plate. The obtained data of each one is investigated individually and compared with each other attempting to conclude an overview of damages presence in the tested component.
The composite material specimen undergoes three different states based on the damage existence in it. In each state, the decay rate is done and the result data is measured. Distinguish the difference in the response of the dynamic behaviour in each case is analysed and considered to indicate the damage existence.

7.2. *Vibration Decay Rate*

Generally, there are several methods for the experimental determination of the damping of materials. One of these methods is the determination of the vibration decay rate, which gives a relatively simple method for the loss factor determination [38].
The measurement of vibration decay rate is pretty like the measurement of the acoustic decay rate, which is well known in the room acoustics. The only difference is the usage of vibration sensor, e.g., accelerometer instead of microphones. The probe whose decay rate is determined, must be excited with a mechanical impulse (e.g., impact hammer) or with a burst random signal (electro-dynamic shaker) and the time signal of the accelerometer on the structure is measured (impulse response). After the stop of the excitation the gradual drop of the acceleration level within a certain time can be observed in the signal. The length of this time is depending on the internal damping of the material [39]. Additional effect, e.g., the noise radiation can act like a damping, but this phenomenon is neglected in this investigation. More details about the decay rate are already provided in section 4.7.

7.3. *Damping of Materials*

Materials have the capacity to extinct the vibration energy which is introduced to them. The reason for this is the internal friction or damping in materials, which can be caused by a variety of combinations of fundamental physical mechanisms, depending upon the specific material.
For metals, these mechanisms include thermo-elasticity on both the micro and macro scales, grain boundary viscosity, point-defect relaxations, eddy-current effects, stress-induced ordering, and electronic effects[39].
For non-metallic materials, such as polymers and elastomers, the physical micro-mechanisms operative is also known, and considerable phenomenological data have been obtained. Due to the long-range molecular order associated with their giant molecules, polymers exhibit rheological behaviour intermediate between that of a crystalline solid and a simple liquid. The damping and stiffness are markedly depending on frequency and temperature.
The loss factors correspond to pure internal damping, thus radiation losses and the damping at the connections of some compounds (e.g. spot-welded connections) must be separately treated [85].
The damping behaviour can be described with several measures; the mainly used are shown below:
Bandwidth of half-power points under steady-state sinusoidal excitation,
Loss tangent under steady-state sinusoidal excitation (tan φ),
Logarithmic decrement (Λ),
Loss factor (η),
Damping ratio (ξ),
Lehr's damping (D) etc.
There are certain interrelationships among these measures, e.g.:

$$\eta = tan\varphi = 2 \cdot \xi = \Lambda / (n \cdot \pi) = (2 \cdot D) / n \qquad (7.1)$$

7.4. *The Relation between Loss Factor and Decay Time*

Damping loss factor gives an indication about the dissipated energy in the structure. It is a dimensionless quantity that defines as the ratio of amount of energy dissipated per radian to the total energy of the system[86]. Or it is the ratio of the power dissipated Dp , the total stored mechanical energy E, and the angular frequency ω [87].

$$\eta(\omega) = Dp / E._{\omega} \qquad (7.2)$$

where ω is the angular frequency where the loss factor calculated.
However, the estimation of the loss factor is also possible by the measurement of vibration decay time RT60.
RT60 is defined as the time at within which the energy of the vibration is reduced to one millionth of its initial value (-60 dB). In other words it could be defined as the time in which the signal level is decreased by 60 dB after the source has been switched off [88].
As mentioned in section 4.7, the filtered RT60 is related to loss factor over the frequency by the following formula [36]:

$$\eta(f) = 2.2 / f \cdot RT_{60} \quad (7.3)$$

where
f: is the mid frequency of a third octave band in Hz.
RT_{60}: is the decay rate for each third octave mid frequency in s.
The value of 2,2 is derived from the energy drop to the one millionth of the initial value.

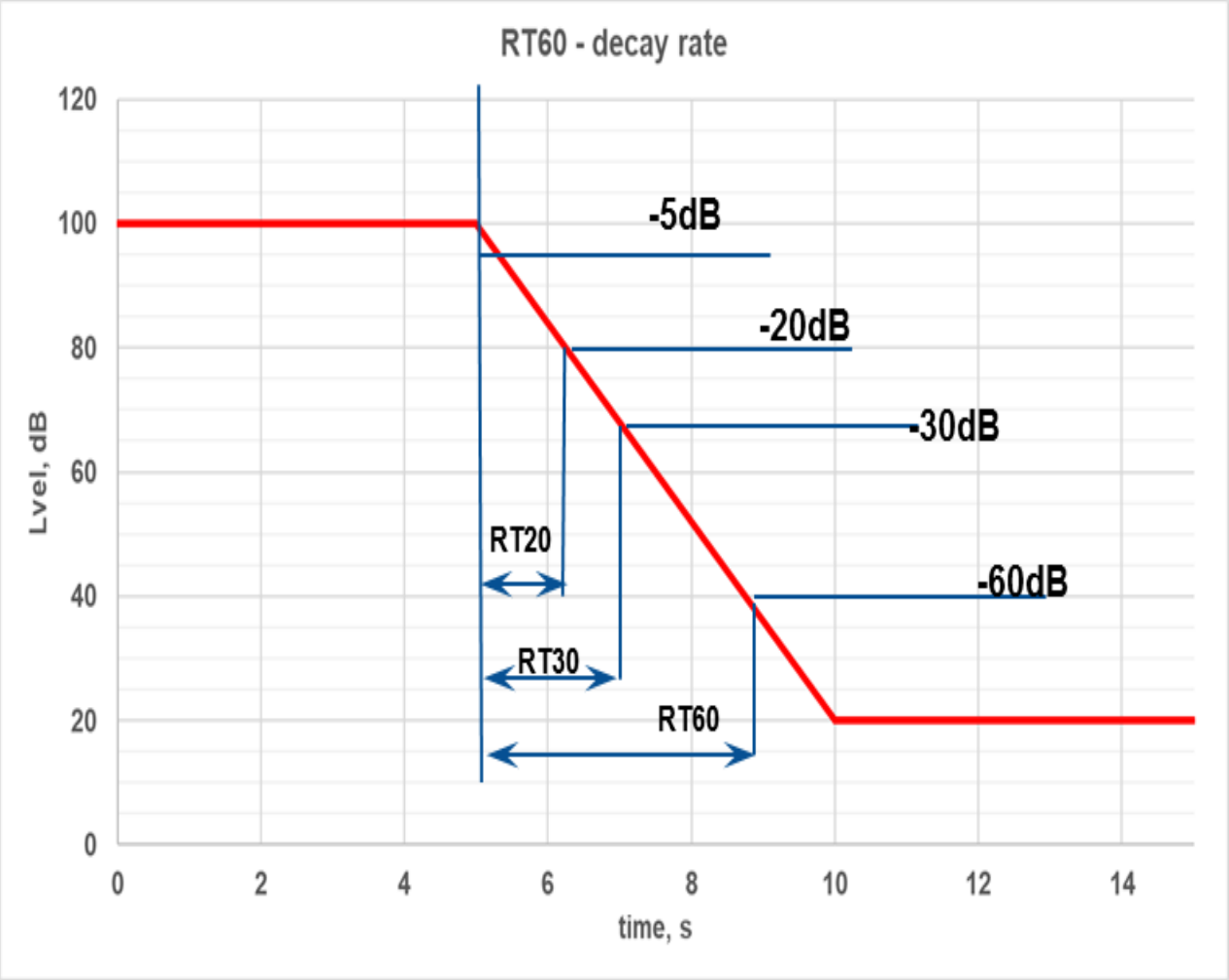

Figure 7. 1. Decay Rate Curve

7.5. *Experimental Work*

7.5.1. The Test Specimen

For the investigations, a material type of MF GC 201 (melamine resin laminate) is selected. It is a glass reinforced polymer that consists of several layers of glass cloth impregnated with melamine. The specimen has a simple rectangular shape with the dimensions of 500 x 200 x 3 mm. The material tensile strength is 150 MPa while the compressive strength is 275 MPa. The modulus of elasticity of the material is 1400 MPa.

7.5.2. Creating Damages in the Specimen

Artificial Damage is created by the same way mentioned in section 6.4. Thus, the specimen was tested three times based on the conditions undamaged, damaged1, and damaged 2.

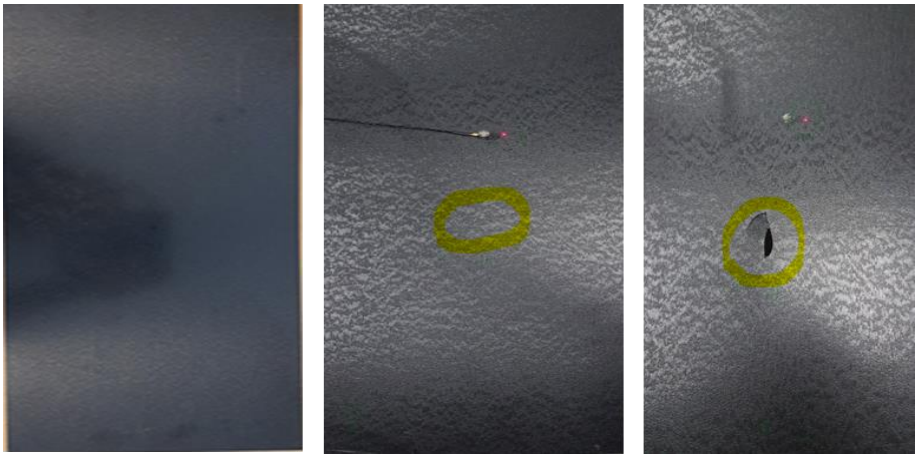

Figure 7. 2. The Test Specimen with Three Conditions.

7.5.3. Test Equipment

- B&K Pulse data acquisition
- B&K 4397 accelerometer
- Impact hammer (hand-made from a B&K 4397 accelerometer)
- The software

The specimen is elastically supported as it is shown in the schematic representation of the test set up which is already explained in figure 4.7 of chapter 4.

7.5.4. Performing the Test

Three excitation points and one measurement point were determined to perform the hits and record the results. The first excitation points is the middle of the specimen, while the second and third were (10, 10) and (3, 5) from the lower edge respectively. The measurement point is horizontally in the middle and vertically in the upper one-third of the part.

As mentioned, the test is done three times according to the three different conditions of the specimen. First time, the specimen is free of damages while the second time the specimen is damaged, but the crack is barely seen by eye supposing that there are damages in the microstructure of the part which may be detected by the resulting signal. The third test is done when the specimen is fully cracked as there is a gap in the spacemen.

During each time of the test, the excitation points are respectively hit ten times by the hammer and the recorded data were averaged. All recorded data are analysed by the Room Acoustic Wizard software and graphs are generated.

7.6. *Test Results*

7.6.1. Vibration Decay Rate

The graph (7.7) shows the RT60 of all three states together. As it is clear in figure 7, over 1000 Hz, there is a big difference can be seen among the three of them. The damaged condition no.2 (grey line) showing the highest RT60 conflicting the fact that a part of the material (a fragment) is missing, so the internal material damping is less. Same fact can be applied to the damaged case no.1 (orange line) considering that there is a crack so there is micro-displacement between the crack surfaces (Coulomb-friction), so the damping is increased compared to the original specimen. In accordance with the results above, the presence of damages can be estimated by the vibration decay rate in specific condition.

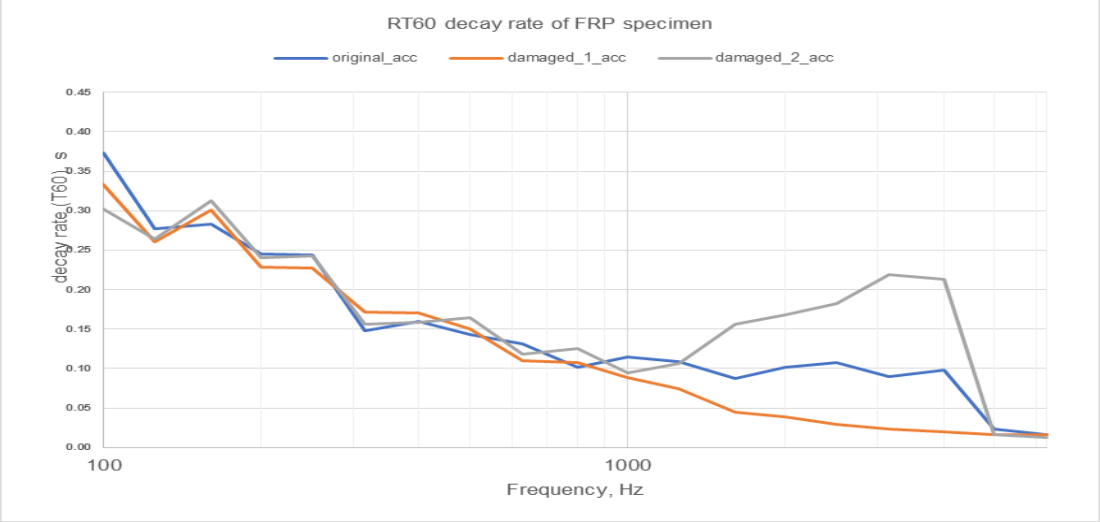

Figure 7. 3. RT 60 Decay Rate of the Three Cases.

7.6.2. The Loss Factor

Figure (8.6) shows the relation of the loss factors for the three different damage conditions of the same specimen. Up to 1000 Hz there is no difference in damping behaviour. Beyond 1000 Hz significant differences of the loss factors can be observed.
The loss factor of the damaged-1 specimen is three times higher as that of the original. The damage-1 condition means only a barely visible crack in the plate, so that micro-sliding occurs. This is producing the Coulomb-friction between the cracked surfaces, which is finally dissipating the vibration energy faster than in the original condition.
In case of damaged-2, material area of (0.5 x 2 cm) is cracked out from the specimen, so this area fragment is practically missing. In this case, over 1000 Hz, the loss factor is roughly half as high as in original condition. Due to the missing material fragment the Coulomb-friction cannot take effect, so the loss factor is reduced. In addition, the missing material fragment means also less internal damping generating micro-mechanisms, with the result of less damping than the original. It is quite surprising, that so small missing part causes a significant drop of the loss factor.

As it is shown in the two graphs that the difference among the three conditions of the specimens are clear over 100 Hz. This can be explained as the modal behaviour (the mode shapes) of the plate is the main reason for that frequency range. As it shown that n this frequency range (1000 - 4000Hz) the mode shapes are affected strongly by the cracks. The dimension of the specimen, the length of the crack, the gab created, and the material type are all causing such frequency ranges because these factors all have influence on the dambing of the materials.

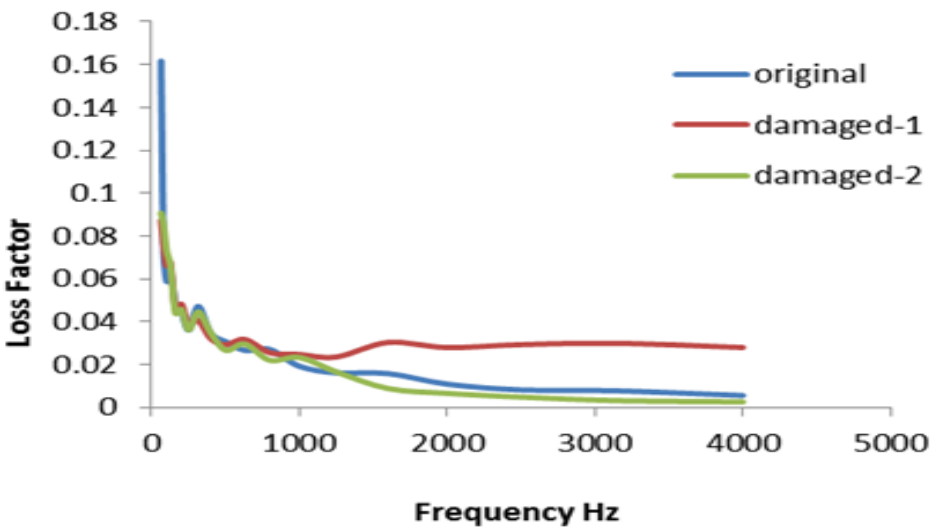

Figure 7. 4. The Loss Factor of the Three Cases.

7.7. *Conclusion*

As the composite materials usage has been significantly increased in major industry fields, the monitoring of damages presence in the composite parts and structure has to take a major importance. The damages in composite materials might exist non-visibly due to fatigue or crack. Thus, acoustic emission methods are used to predict damages existence in composite structure. Vibration decay rate is an acoustic method that has been used in this experimental investigation. The investigation used a composite material specimen that is made of glass fiber reinforced polymer. The specimen is put under three different damage conditions. The first is free of damages and the other two are different damage levels. The measured RT60 showed a clear difference after 1000 Hz of frequency between all three cases proving that this method is able to estimate the presence of damages in the part.

The damping response is studied under three different conditions based on damage existence. Firstly, the plate is investigated as free of damages. After that, two artificial damages are made respectively in the plate and studied separately.

The loss factor is measured for all cases to determine whether there is difference among them in order to prove damage presence in the composite part. The measurement of the loss factor is experimentally done by evaluating the vibration decay time RT60. A well-distinguished difference is revealed by the resulted data proving the difference occurring by the damages of the plate. The results may lead to expand the research by focusing on the location and identity of the damages.

8. MODAL ANALYSIS OF PRE-TENSILE-LOADED COMPOSITE PLATES

8.1. *Introduction*

The goal of the investigation was to determine the modal behaviour of the specimen with different preload condition, resp. with different material damage condition resulting from the tensile loading. Two specimens with different geometry were used for the tests. The first one was a probe with 250x25x3 mm dimensions, the second was slightly different, with the same surface area but with 5 mm thickness. The specimen was put into a tensile pull machine and was loaded with different loads. The 3 mm thick probes were loaded with forces, which caused 2 mm, 4 mm and 6 mm length extension. The 4th probe was kept unloaded; it served as the reference probe. Similar to that the 5 mm thick probes were also loaded, with 2,5 mm, 5 mm and 7,5 mm length extension of the probes. The 4th was kept unloaded. After loading the probes, the force was released, so the probes could take their unloaded length. The goal of the tensile loads was to create damages inside material structure of the probes.

8.2. *Experimental Work*

8.2.1. Specimen

Two composite plates of (250x25x5) mm and (250x25x3) mm were used in this test. The plates are made of glass fiber reinforcing epoxy resin. The specimens were provided by Quattroplast Hungary Company.

Table 8. 1. The Material Technical Data Sheet (Quattroplast Company).

Property	Unit	Method	Value
Density	g/cm^3	DIN EN ISO 1183	1.9
Flexural modulus	MPa	ISO 178	24000
Tensile strength (parallel)	MPa	ISO 527	300
Compressive strength (perpendicular)	MPa	ISO 604	350
Flexural stress at rupture (perpendicular)	MPa	ISO 178	340
Interlaminar resistance	N	DIN 53463	3000
Compressive strength (parallel)	MPa	ISO 604	180
Impact strength, Charpy (parallel)	kJ/m^2	ISO 179	33

8.2.2. Measurement Setup

The probes were put onto a TIRA TV 50009 electrodynamic vibration test system (shaker) as shown in figure 8.1. The shaker can provide a 9 N excitation force as maximum. The probes were mounted sequentially on the shaker interconnected with a PCB 288D01 impedance head. The probes were glued on the mounting plate of the impedance head with HBM X60 two components cold curing glue at the half length of the probes. With the impedance head the exciting force and the vibrational acceleration at the exciting point could be measured.
Roughly 90 mm from the middle of the probe (only one side) a reflective patch was fixed on the probe surface. At this point the vibration of the probe due to the excitation was measured with an out of plane laser doppler vibrometer Ometron VH-1000 (B&K 8338).
The measured signals (force, acceleration, velocity) were connected to a 4 channel DAQ (B&K Photon +). The measurement software created the desired functions, in this case the frequency response functions (FRF) between force and acceleration ($m/s^2/N$) and force and velocity (m/s/N), the coherences for each FRFs. The FRF acceleration over force (a/F) is called inertance, the velocity over force (v/F) is called mobility.

Figure 8. 1. The Test Set Up.

8.3. *Results and Discussion*

The FRF functions, inertance and mobility were represented in diagrams for each probe (Figure 8.2). The curves are showing the resonance frequencies of the probes. Additionally, a FEM model of the probe was created and FEM calculations were performed in order to determine the mode shapes for each resonance frequency. (Performing the FEM calculation was easier and faster than to perform a measurement, since for the measurement roughly 40 points had to be measured sequentially on the probe to represent the probe geometry with a proper accuracy.)

The FRRs are showing that the resonance frequencies of the unloaded probe have higher frequency resonances than the loaded ones. The differences in frequencies for each resonance (for unloaded and max. loaded (7,5 mm) probe) are the following (Table 8.1):

Table 8. 2. Differences of the Resonance Frequencies of the Unloaded and Max. loaded Probe of (5mm Thickness).

Nr.	Unloded probe	Max. loaded probe	Difference
1.	323 Hz	311 Hz	12 Hz
2.	1635 Hz	1615 Hz	23 Hz
3.	4054 Hz	3910 Hz	144 Hz
4.	7525 Hz	7128 Hz	398 Hz
5.	11466 Hz	10938 Hz	528 Hz
6.	15915 Hz	15280 Hz	635 Hz

The results are showing that the damage of the probe material due to external loading through a tensile test machine has a significant effect on the resonance frequencies of the probes. It means that the probes behave less stiff as in unloaded condition. This behaviour can be explained through the damage of the matrix or the glass fiber. Which of them, resp. in which dimension is responsible for the stiffness falling can only be explained with CT tests which is shown in the next chapter.

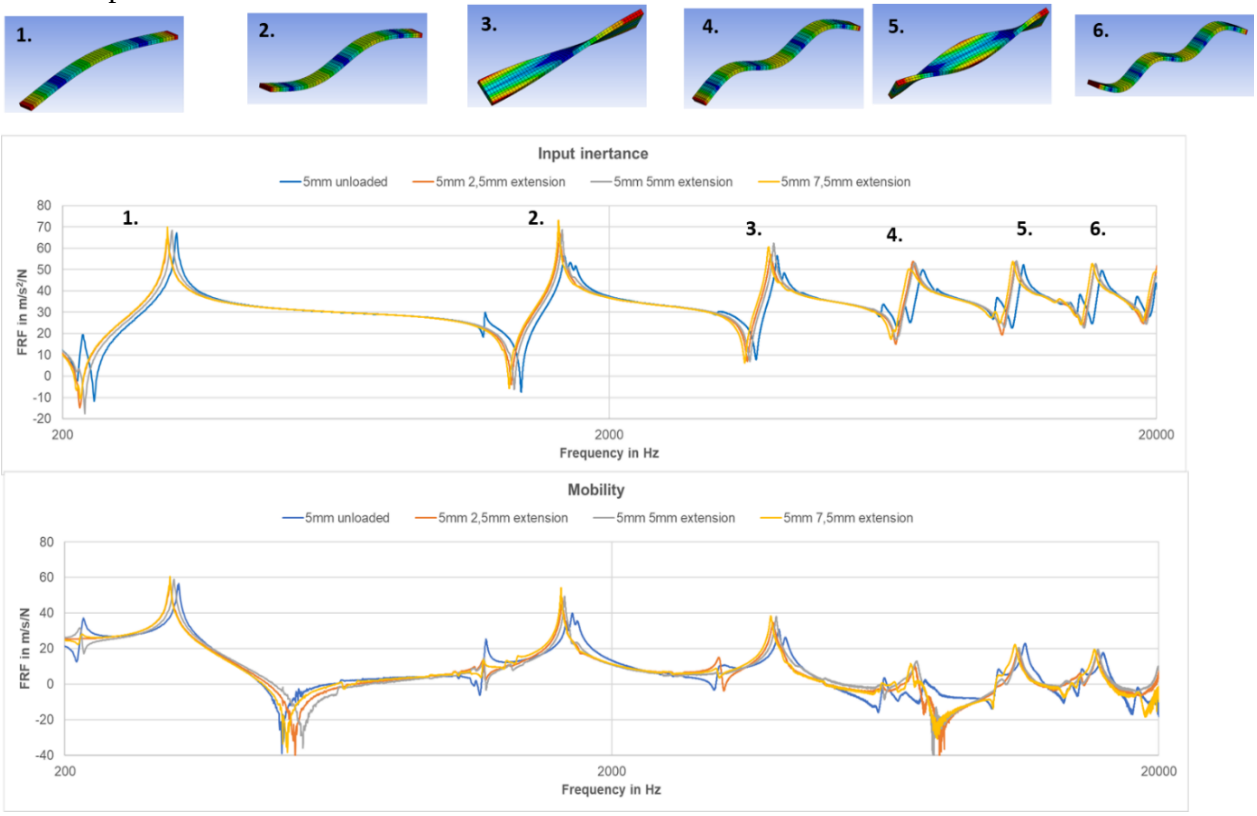

Figure 8. 2. The Resonance Frequencies of the First Specimen (5mm thick).

Going upwards in the frequency axis the mode shapes became more and more complex. The global modes (e.g., the first bending mode) are less affected; the more complex modes are more affected from the internal material damage.
The above-described behaviour also can be noticed for the probes with less extension (2,5 mm and 5 mm), of course with less difference in the resonance frequencies.

8.4. *Computed Tomography (CT) Scanning of the Specimen*

Figure 8.3 shows some CT scan views of the specimen. In order to figure out the change in the microstructure, the focus was on the woven fabric in the front view.
At First sight, it is not clear that there is flaw or defect in the material constituents between the unloaded and the loaded cases of the specimen. Thus, to invistigate more deeply, Distances between every two points of the woven fabric of the unloaded and the maximum loaded specimen are measured.

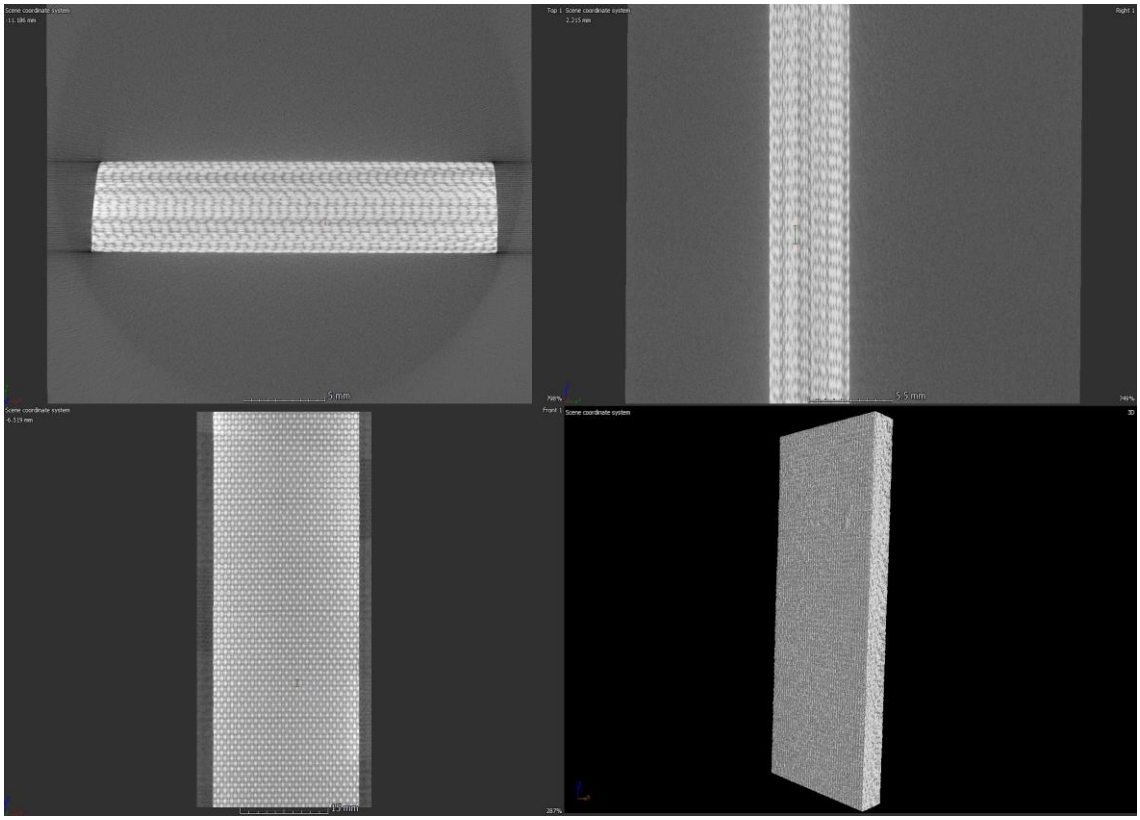

Figure 8. 3. CT Scanning Views of the Specimen.

The results show that approximately the distances between the points in the woven fiber of the microstructure image in the unloaded case is 1.004 mm while in the max loaded case is 1.57 mm as it shown in figure 8.4.
This could be also an indication of the damage effect because there is a different displacement between the measured points of two specimens. It might be an indication of beginning of damage such as fiber matrix debonding or delamination.
Although there is very slight displacement between the woven fibers, it is clear that the modal analysis method is more sensitive to detect such damages.

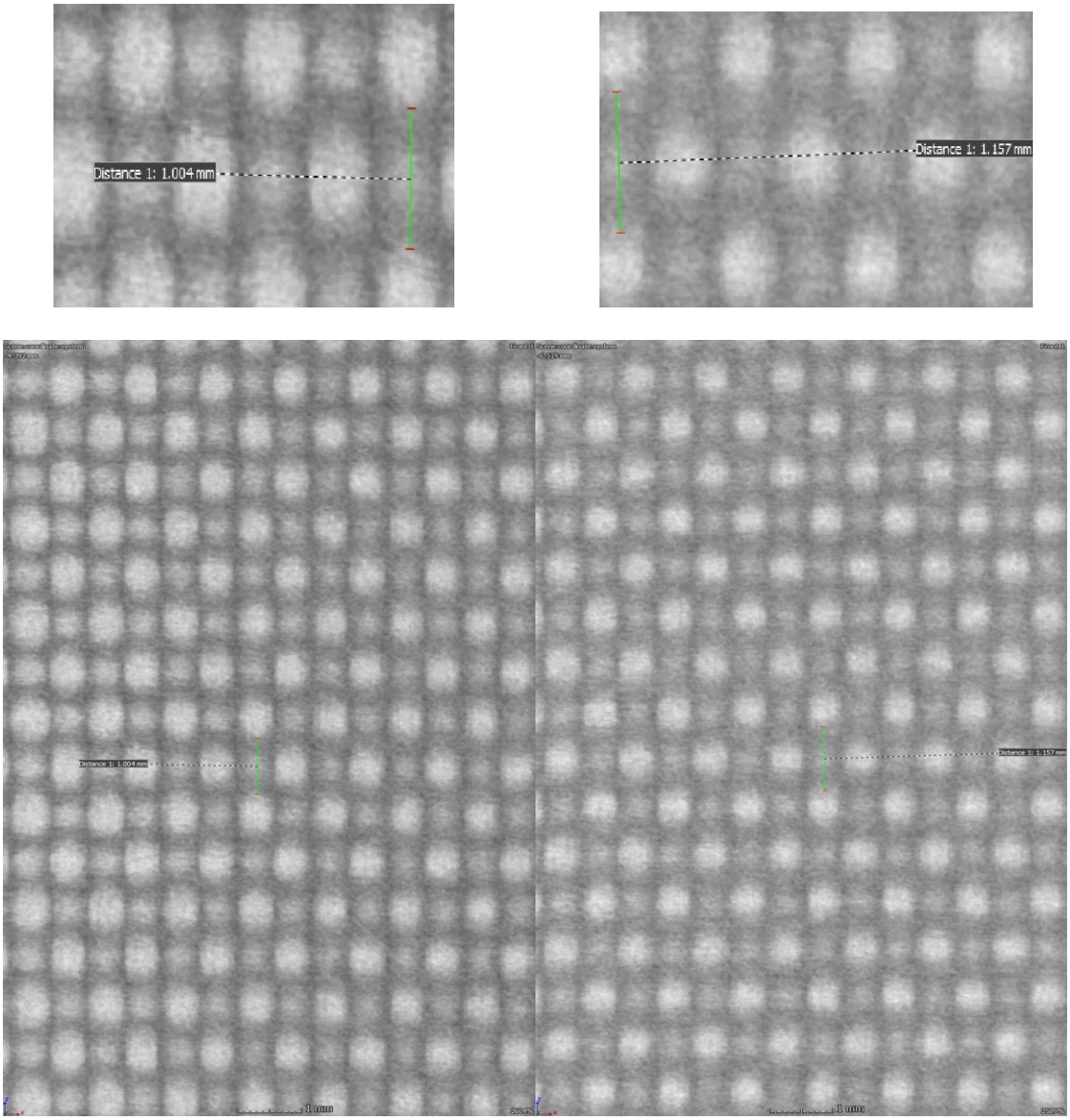

Figure 8. 4. Distance Between the Tow Points of the Woven Fiber in the Specimens (left: unloaded), (right: the max.loaded).

8.5. *Conclusions*

The modal behavior of glass fiber reinforced epoxy specimen with different pre-tensile loaded conditions is studied. The found results show that the damage of the probe material due to external tensile loading has a significant effect on the resonance frequencies of the probes. The probes behave less stiff as in unloaded condition. This behavior can be explained through the damage of the matrix or the glass fiber. CT scan is done to the specimens and the results shows an indication of damge in materials becasue there is slight displacemet between the woven fiber which can be explained as begining of fiber delamination or fiber matrix debonding. It is clearly indicated in this investigation that the modal analysis method is more sensitive to detect such damages.

9. THESIS

1. I used particle swarm optimization (PSO) to find the best design parameters including spatial elements of the unit cell as well as a given set of strength values for both Glass-fiber and Epoxy. A comparative study is done to select optimal fiber diameter that can satisfy the optimal longitudinal tensile strength. Thus, I proved that PSO was efficient enough to find the best possible design parameters within only five iterations [K2].

2. I used the micromechanical theories to prove that the longitudinal modulus E_1 is increasing with the increase of fiber volume fraction. Also, there is a linear increment of the transverse modulus E_2 with the increment of fiber volume fraction. In addition, in plane Shear modulus G_{12} increases linearly with increase in fiber volume fraction for all the three types of glass fibers. However, for all composites, Poisson's ratio V_{12} is decreasing with increasing the fiber volume fraction. The investigation is done on three types of glass fibers reinforced polymer lamina [K5].

3. I investigated the noise, vibration, and harshness (NVH) behavior of damaged and not damaged fiber reinforced polymer FRP plate by using the modal analysis method. The results that we found showed that the modal analysis is an effective tool for detecting such damages because it is clearly observed that the method is sensitive of to the damage existence. Also, it is indicated that there are changes in the NVH characteristics of the specimens due to the damages [K1].

4. I experimentally used the vibration decay rate as a method to detect damages in a FRP component. Measurement of reverberation time RT60 is executed in three different damage conditions of a specimen made of fiber reinforced polymer. I proved that the method is able to estimate the presence of damages in the part as the measured RT60 showed a clear difference over 1000 Hz of frequency between all three cases (undamaged / damaged 1/ damaged 2) specimens [K4].

5. I investigated the damping response offered by a damaged fiber reinforced polymer plate. The plate is elastically supported and put under three different conditions regarding the damage existence. I found that the loss factor of the damaged-1 specimen is three times higher than that of the original. In case of damaged-2, over 1000 Hz, the loss factor is roughly half as high as in the original condition. In my investigation, I found that the damping behavior of the composite specimen gives clear indication about the damage status of the material [K6].

6. I studied the modal behavior of glass fiber reinforced epoxy specimen with different pre tensile-loaded conditions. The results I found show that the damage of the probe material due to external tensile loading has a significant effect on the resonance frequencies of the probes. I proved, that the probes behave less stiff as in unloaded condition. This behavior can be explained as that the load has caused damage in the matrix or in the reinforcement part or in both.

REFERENCES

1. Rajak DK, Pagar DD, Menezes PL, Linul E (2019) Fiber-reinforced polymer composites: Manufacturing, properties, and applications. Polymers (Basel) 11:1667. https://doi.org/10.3390/polym11101667
2. Alberto M (2013) Introduction of Fibre-Reinforced Polymers − Polymers and Composites: Concepts, Properties and Processes. In: Fiber Reinforced Polymers - The Technology Applied for Concrete Repair
3. Goh GD, Yap YL, Agarwala S, Yeong WY (2019) Recent Progress in Additive Manufacturing of Fiber Reinforced Polymer Composite. Adv Mater Technol 4:1800271. https://doi.org/10.1002/admt.201800271
4. Zindani D, Kumar K (2019) An insight into additive manufacturing of fiber reinforced polymer composite. Int J Light Mater Manuf. 2(4):267-78 https://doi.org/10.1016/j.ijlmm.2019.08.004
5. Ozbakkaloglu T, Chen JF, Smith ST, Dai JG (2016) Applications of Fiber Reinforced Polymer Composites. Int. J. Polym. Sci.
6. Günaslan SE, Karaşin A, Öncü ME (2014) Properties of FRP materials for strengthening. Int J Innov Sci Eng Technol. 1(9):656-60
7. Jollivet T, Peyrac C, Lefebvre F (2013) Damage of composite materials.Procedia Engineering. 66:746-58
8. Razali N, Sultan MTH, Mustapha F, et al (2014) Impact Damage on Composite Structures – A Review. Int J Eng Sci. 3(7):08-20
9. Ghobadi A (2017) Common Type of Damages in Composites and Their Inspections. World J Mech. 7(2):24-33 https://doi.org/10.4236/wjm.2017.72003
10. Heslehurst RB (2014) Defects and Damage in Composite Materials and Structures. CRC press, Boca Raton, FL, USA
11. Ngo T-D (2020) Introduction to Composite Materials. In: Composite and Nanocomposite Materials - From Knowledge to Industrial Applications
12. Reddy Nagavally R (2017) COMPOSITE MATERIALS-HISTORY, TYPES, FABRICATION TECHNIQUES, ADVANTAGES, AND APPLICATIONS. Int J Mech Prod Eng 5:28–7
13. Johnson T (2018) History of Composites. Evol Light Compos. Mater.
14. Ashby MF, Cebon D (1993) Materials selection in mechanical design. J Phys 3:1–9. https://doi.org/10.1051/jp4:1993701
15. Kashtalyan M (2018) Introduction to Composite Materials Design– Third editionE. J. Barbero CRC Press, Taylor & Francis Group, 6000 Broken Sound Parkway NW, Suite 300, Boca Raton, FL, 33487-2742, USA. 2018. Distributed by Taylor & Francis Group, 2 Park Square, Milton Park, Ab. Aeronaut J. https://doi.org/10.1017/aer.2018.135
16. Fleischer J, Teti R, Lanza G, et al (2018) Composite materials parts manufacturing. CIRP

Ann. 67(2):603-26
https://doi.org/10.1016/j.cirp.2018.05.005
17. Arredondo SP, Corral R, Valenciano A, et al (2022) Strength, Elastic Properties and Fiber–Matrix Interaction Mechanism in Geopolymer Composites. Polymers (Basel) 14:. https://doi.org/10.3390/polym14061248
18. Zweben C (2006) Composite Materials. In: Mechanical Engineers' Handbook: Materials and Mechanical Design, Third Edition
19. Thomas, S., Joseph, K., Malhotra, S.K., Goda, K. and Sreekala, M.S. eds., 2012. Polymer composites, macro-and microcomposites (Vol. 1). John Wiley & Sons
20. Fu SY, Feng XQ, Lauke B, Mai YW (2008) Effects of particle size, particle/matrix interface adhesion and particle loading on mechanical properties of particulate-polymer composites. Compos Part B Eng. 39(6):933-61
https://doi.org/10.1016/j.compositesb.2008.01.002
21. Massoumi B, Mohammad-Rezaei R, Abbasian M, Jaymand M (2019) Amine-functionalized carbon nanotubes as curing agent for polystyrene-modified novolac epoxy resin: synthesis, characterization and possible applications. Appl. Phys. A Mater. Sci. Process. 125(5):1-7
22. Divya H V, Naik LL, Yogesha B (2016) Processing Techniques of Polymer Matrix Composites – A Review. Int J Eng Res Gen Sci Vol 4:357–362
23. M K Lila, U K Komal IS (2016) Secondary Processing of Polymer Matrix Composites: Challenges and Opportunities. In: International Conference on Latest Development in Material, Manufacturing and Quality Control, MMQC-2016
24. De Luca A, Caputo F (2017) A review on analytical failure criteria for composite materials. AIMS Mater Sci.4(5): 1165-1185
https://doi.org/10.3934/matersci.2017.5.1165
25. Cantwell WJ, Morton J (1992) The significance of damage and defects and their detection in composite materials: A review. J Strain Anal Eng Des. 27(1):29-42
https://doi.org/10.1243/03093247V271029
26. Tang JM, Lee WI, Springer GS (1987) Effects of Cure Pressure on Resin Flow, Voids, and Mechanical Properties. J Compos Mater. 21(5):421-40
https://doi.org/10.1177/002199838702100502
27. Van Dreumel WH m., Kamp JL m. (1977) Non Hookean Behaviour in the Fibre Direction of Carbon-Fibre Composites and the Influence of Fibre Waviness on the Tensile Properties. J Compos Mater. 11(4):461-9
https://doi.org/10.1177/002199837701100408
28. Hou W, Zhang W (2012) Advanced composite materials defects/damages and health monitoring. In: Proceedings of IEEE 2012 Prognostics and System Health Management Conference, PHM-2012.(pp1-5)
29. Liu D (1988) Impact-Induced Delamination—A View of Bending Stiffness Mismatching. J Compos Mater. 22(7):674-92
https://doi.org/10.1177/002199838802200706
30. Renard J (2010) Fatigue des matériaux composites renforcés de fibres continues. Tech l'Ingénieur
31. Talreja R, Varna J (2015) Modeling damage, fatigue and failure of composite materials. Elsevier
32. Meola C, Toscano C (2012) NonDestructive Evaluation of Carbon Fiber Reinforced Polymers with Ultrasonics and Infrared Thermography: An Overview on Historical Steps and Patents. Recent Patents Mater Sci. 5(1):48-67
https://doi.org/10.2174/1874465611205010048
33. Meola C, Boccardi S, Carlomagno GM (2016) Infrared Thermography in the Evaluation

of Aerospace Composite Materials: Infrared Thermography to Composites. Woodhead Publishing
34. Kaiser H, Karbhari VM, Sikorsky C (2004) Non-destructive testing techniques for FRP rehabilitated concrete - II: An assessment. Int J Mater Prod Technol. 21(5):385-401 https://doi.org/10.1504/IJMPT.2004.004997
35. Shoja S, Berbyuk V, Boström A (2018) Delamination detection in composite laminates using low frequency guided waves: Numerical simulations. Compos Struct. 203: 826-834 https://doi.org/10.1016/j.compstruct.2018.07.025
36. Gresil M, Poohsai A, Chandarana N (2017) Guided Wave Propagation and Damage Detection in Composite Pipes Using Piezoelectric Sensors. In: Procedia Engineering 188: 148-155
37. Alsarayefi S (2020) Damage Detection in a Fibre Reinforced Polymer Component by the Vibration Decay Rate. J Adv Res Dyn Control Syst. 12(SP8):644-50 https://doi.org/10.5373/jardcs/v12sp8/20202566
38. Petrone G, D'Alessandro V, Franco F, De Rosa S (2015) Damping evaluation on eco-friendly sandwich panels through reverberation time (RT 60) measurements. JVC/Journal Vib Control 21:3328–3338. https://doi.org/10.1177/1077546314522507
39. Fahy F (2003) Foundations of Engineering Acoustics
40. Chen YM, Liu QX, Liu JK (2019) Time-Dependent Decay Rate and Frequency for Free Vibration of Fractional Oscillator. J Appl Mech Trans ASME. 86(2):024501 https://doi.org/10.1115/1.4041824
41. Romhány G, Czigány T, Karger-Kocsis J (2017) Failure Assessment and Evaluation of Damage Development and Crack Growth in Polymer Composites Via Localization of Acoustic Emission Events: A Review. Polym. Rev.57(3):397-439
42. Pinho ST, Pimenta S (2014) Size Effects on the Strength and Toughness of Fibre–Reinforced Composites. Proc 10th World Congr Comput Mech 1:4394–4413. https://doi.org/10.5151/meceng-wccm2012-19865
43. Ramsteiner F, Theysohn R (1985) The influence of fibre diameter on the tensile behaviour of short-glass-fibre reinforced polymers. Compos Sci Technol 24:231–240. https://doi.org/10.1016/0266-3538(85)90075-2
44. Çuvalci H, Erbay K, İpek H (2014) Investigation of the Effect of Glass Fiber Content on the Mechanical Properties of Cast Polyamide. Arab J Sci Eng 39:9049–9056. https://doi.org/10.1007/s13369-014-1409-8
45. Landesmann A, Seruti CA, Batista EDM (2015) Mechanical properties of glass fiber reinforced polymers members for structural applications. Mater Res 18:1372–1383. https://doi.org/10.1590/1516-1439.044615
46. Alsarayefi SJ, Jalics K (2019) The change of the NVH characteristics of composite vehicle components as a result of visible and not visible damages. In: Advances and Trends in Engineering Sciences and Technologies III- Proceedings of the 3rd International Conference on Engineering Sciences and Technologies, ESaT 2018, (p. 9). CRC Press
47. Kim J-W, Kim H-S, Lee D-G (2012) Tensile Strength of Glass Fiber-Reinforced Plastic By Fiber Orientation and Fiber Content Variations. Int J Mod Phys Conf Ser 06:640–645. https://doi.org/10.1142/s201019451200390x
48. Cookson MD, Stirk PMR (2019) Vibro-Acoustic Simulation of Aluminium Foam Parts Using MultiScale Techniques. Adv Eng Mater 13:1015–1018
49. Drugan WJ, Willis JR (1996) A micromechanics-based nonlocal constitutive equation and estimates of representative volume element size for elastic composites. J Mech Phys Solids 44:497–524. https://doi.org/10.1016/0022-5096(96)00007-5

50. Mori T, Tanaka K (1973) Average stress in matrix and average elastic energy of materials with misfitting inclusions. Acta Metall 21:571–574. https://doi.org/10.1016/0001-6160(73)90064-3
51. Eshelby JD (1957) The determination of the elastic field of an ellipsoidal inclusion, and related problems. Proc R Soc London Ser A Math Phys Sci 241:376–396
52. Melro AR, Camanho PP, Andrade Pires FM, Pinho ST (2013) Micromechanical analysis of polymer composites reinforced by unidirectional fibres: Part II-Micromechanical analyses. Int J Solids Struct 50:1906–1915. https://doi.org/10.1016/j.ijsolstr.2013.02.007
53. Evans JT (1992) Analysis and performance of fiber composites (second edition)
54. Yang QS, Qin QH (2004) Micro-mechanical analysis of composite materials by BEM. Eng Anal Bound Elem 28:919–926. https://doi.org/10.1016/S0955-7997(03)00118-8
55. Wang, A. S. D. "Micromechanics analysis of composite materials." Mechanics of Composite Materials and Structures. Springer, Dordrecht, 1999. 81-130.
56. Zeman J (2000) Micromechanical Analysis of Random Composites
57. Syed Altaf Hussain BSR and VNR (2008) PREDICTION OF ELASTIC PROPERTIES OF FRP COMPOSITE LAMINA FOR LONGITUDINAL LOADING. ARPN J Eng Appl Sci. 3: 70-75
58. Babu KS, Rao KM, Raju VRC, et al (2008) Micromechanical analysis of FRP hybrid composite lamina for in-plane transverse loading. Indian J Eng Mater Sci 15:382–390
59. Barbero EJ (2011) Introduction to Composite Materials Design 2nd ed - Ever J. Barbero (CRC, 2011)
60. Sathishkumar TP, Satheeshkumar S, Naveen J (2014) Glass fiber-reinforced polymer composites - A review. J. Reinf. Plast. Compos. 33(13):1258-75
61. Karbhar VM, Kaiser H, Navada R, et al (2005) Methods for detecting defects in composite rehabilitated concrete structures. (No. FHWA-OR-RD-05-09)
62. Heylen W, Lammens S, Sas P (1998) Modal Analysis Theory and Testing, 2nd ed. Belgium : Katholieke Universiteit Leuven, Faculty of Engineering, Dept. of Mechanical Engineering, Division of Production Engineering, Machine Design and Automation
63. dos Santos FLM, Peeters B, Van der Auweraer H, et al (2016) Vibration-based damage detection for a composite helicopter main rotor blade. Case Stud Mech Syst Signal Process. 3:22-7 https://doi.org/10.1016/j.csmssp.2016.01.001
64. Katunin A (2013) Modal-Based Non-Destructive Damage Assessment in Composite Structures Using Wavelet Analysis: A Review. Int J Compos Mater.3(6B):1-9 https://doi.org/10.5923/201310.01
65. Katunin A (2014) 1471. Damage assessment in composite structures using modal analysis and 2D undecimated fractional wavelet transform. J Vibroengineering. 16(8):3939-50
66. Lakhdar M, Mohammed D, Boudjemâa L, et al (2013) Damages detection in a composite structure by vibration analysis. Energy Procedia.36:888-97
67. Yelve NP, Mitra M, Mujumdar PM (2017) Detection of delamination in composite laminates using Lamb wave based nonlinear method. Compos Struct. 159:257-66 https://doi.org/10.1016/j.compstruct.2016.09.073
68. Pérez MA, Gil L, Oller S (2014) Impact damage identification in composite laminates using vibration testing. Compos Struct. 108:267-76 https://doi.org/10.1016/j.compstruct.2013.09.025
69. Kessler SS, Spearing SM, Atalla MJ, et al (2002) Damage detection in composite materials using frequency response methods. Compos Part BEngineering. 33(1):87-95 https://doi.org/10.1016/S1359-8368(01)00050-6
70. Sadarang J, Nayak S, Nayak G, et al (2018) Dynamic analysis for delamination detection

in carbon fiber composite beam. IOP Conf Ser Mater Sci Eng 402: https://doi.org/10.1088/1757-899X/402/1/012143
71. Vo-Duy T, Ho-Huu V, Dang-Trung H, et al (2016) Damage detection in laminated composite plates using modal strain energy and improved differential evolution algorithm. In: Procedia Engineering. Elsevier Ltd, pp 182–189
72. Fan W, Qiao P (2011) Vibration-based damage identification methods: A review and comparative study. Struct. Heal. Monit. 10(1):83-111
73. Carden EP, Fanning P (2004) Vibration based condition monitoring: A review. Struct. Heal. Monit. 3(4):355-77
74. Oruganti K, Mehdizadeh M, John S, Herszberg I (2008) Vibration-based analysis of damage in composites. In: Materials Forum. Vol. 33, p. 496
75. Zhang Z, He M, Liu A, et al (2018) Vibration-based assessment of delaminations in FRP composite plates. Compos Part B Eng. 144:254-66 https://doi.org/10.1016/j.compositesb.2018.03.003
76. Montalvão D, Maia NMM, Ribeiro AMR (2006) A review of vibration-based structural health monitoring with special emphasis on composite materials. Shock Vib. Dig. 38(4):295-324
77. Yam LH, Yan YJ, Jiang JS (2003) Vibration-based damage detection for composite structures using wavelet transform and neural network identification. Compos Struct. 60(4):403-12 https://doi.org/10.1016/S0263-8223(03)00023-0
78. Zou Y, Tong L, Steven GP (2000) Vibration-based model-dependent damage (delamination) identification and health monitoring for composite structures - a review. J Sound Vib. (2):357-78 https://doi.org/10.1006/jsvi.1999.2624
79. Treviso A, Van Genechten B, Mundo D, Tournour M (2015) Damping in composite materials: Properties and models. Compos Part B Eng 78:144–152. https://doi.org/10.1016/j.compositesb.2015.03.081
80. Chandra R, Singh SP, Gupta K (1999) Damping studies in fiber-reinforced composites - a review. Compos Struct.46(1):41-51 https://doi.org/10.1016/S0263-8223(99)00041-0
81. Finegan IC, Gibson RF (1999) Recent research on enhancement of damping in polymer composites. Compos Struct.44:89-98. https://doi.org/10.1016/S0263-8223(98)00073-7
82. Benchekchou B, Coni M, Howarth HVC, White RG (1998) Some aspects of vibration damping improvement in composite materials. Compos Part B Eng. 29(6):809-17 https://doi.org/10.1016/S1359-8368(98)00024-9
83. Berthelot JM, Assarar M, Sefrani Y, Mahi A El (2008) Damping analysis of composite materials and structures. Compos Struct 85:189–204. https://doi.org/10.1016/j.compstruct.2007.10.024
84. Chen J, Liu W, Liu W (2018) Experimental study on vibration decay rate characteristics and improvement for beijing metro. In: Environmental Vibrations and Transportation Geodynamics,2016 (pp. 207-217)
85. Botelho EC, Campos AN, De Barros E, et al (2005) Damping behavior of continuous fiber/metal composite materials by the free vibration method. Compos Part B Eng 37:255–263. https://doi.org/10.1016/j.compositesb.2005.04.003
86. Cherif R, Chazot JD, Atalla N (2015) Damping loss factor estimation of two-dimensional orthotropic structures from a displacement field measurement. J Sound Vib.356:61-71 https://doi.org/10.1016/j.jsv.2015.06.042
87. Cremer L, Heckl M, Petersson BAT (2013) Structure-borne sound: Structural vibrations and sound radiation at audio frequencies. Springer Science & Business Media.
88. Nowoświat A, Olechowska M (2017) Estimation of Reverberation Time in Classrooms

Using the Residual Minimization Method. Arch Acoust 42:609–617. https://doi.org/10.1515/aoa-2017-0065
89. Topa MD, Toma N, Kirei BS, et al (2012) Experimental acoustic evaluation of an auditorium. Adv Acoust Vib 2012:1–9. https://doi.org/10.1155/2012/868247

LIST OF PUBLICATIONS RELATED TO THE TOPIC OF THE RESEARCH FIELD

K1. Alsarayefi, S. J., and Jalics. K. "The change of the NVH characteristics of composite vehicle components as a result of visible and not visible damages." In *Advances and Trends in Engineering Sciences and Technologies III: Proceedings of the 3rd International Conference on Engineering Sciences and Technologies (ESaT 2018), September 12-14, 2018, High Tatras Mountains, Tatranské Matliare, Slovak Republic*, p. 9. CRC Press, 2019.

K2. Alsarayefi, S., Gafil, H.N. and Jalics. K. "Optimization of the fiber size for a fiber glass epoxy composite." *Design of Machines and Structures* 9, no. 1 (2019): 5-12.

K3. Alsarayefi, S., and Jalics. K. "Application of Experimental Modal Analysis to Investigate Damage to Fiber Reinforced Composites." *Multidisciplinary Sciences* 9, no. 4 (2019): 275-282.

K4. Alsarayefi, S., and Jalics. K. "Damage Detection in a Fiber Reinforced Polymer Component by the Vibration Decay Rate." *JOURNAL OF ADVANCED RESEARCH IN DYNAMICAL AND CONTROL SYSTEMS* 12, no. SP8 (2020): 644-650.

K5. Alsarayefi, S., and Jalics. K. "Micromechanical Analysis of Glass Fiber/Epoxy Lamina." In *Vehicle and Automotive Engineering*, pp. 101-111. Springer, Singapore, 2020.

K6. Alsarayefi, S., and Jalics. K. "Anticipation of damage presence in a fiber reinforced polymer plate through damping behavior." *Engineering Solid Mechanics* 9, no. 3 (2021): 263-270.

K7. Alsarayefi, S., and Jalics. K. "Kísérleti modális elemzés alkalmazása szálerősítéses kompozitok károsodásának vizsgálatához." *Multidiszciplináris Tudományok* 9, no. 4 (2019): 275-282.